

DEVELOPMENT OF TESTING PROTOCOLS FOR
DIRECT MEASUREMENTS OF CONTACT ANGLES
ON AGGREGATE AND ASPHALT BINDER
SURFACES USING A SESSILE DROP DEVICE

By

MURAT KOC

Bachelor of Science in Civil Engineering

Bogazici University

Istanbul, Turkey

2010

Submitted to the Faculty of the
Graduate College of the
Oklahoma State University
in partial fulfillment of
the requirements for
the Degree of
MASTER OF SCIENCE
May, 2013

DEVELOPMENT OF TESTING PROTOCOLS FOR
DIRECT MEASUREMENTS OF CONTACT ANGLES
ON AGGREGATE AND ASPHALT BINDER
SURFACES USING A SESSILE DROP DEVICE

Thesis Approved:

Dr. Rifat Bulut

Thesis Adviser

Dr. Stephen A. Cross

Dr. Gregory G. Wilber

ACKNOWLEDGEMENTS

I would like express my most sincere gratitude to my advisor Prof. Rifat Bulut, for his enthusiasm, his encouragement, and his endless support in my graduate education and research studies. His wisdom and guidance helped me to finish my M.S. degree.

I would like to thank all of my family members for their love and support in every field of my life.

I am also indebted to my committee members, Prof. Stephen A. Cross and Prof. Gregory G. Wilber. I owe most of my knowledge about this thesis subject to their lectures and tutoring.

I would like to thank to Prof. James Puckette from Geology Department at Oklahoma State University for letting me use his lab facilities.

My lab friends Aditya Rayudu and Anjana Thoroppady Kittu helped me in many steps of the laboratorial work. I appreciate their help and wish them good luck in their graduate educations.

Last but not the least; I want to thank the Oklahoma Transportation Center for their financial support in this project.

Name: MURAT KOC

Date of Degree: MAY, 2013

Title of Study: DEVELOPMENT OF TESTING PROTOCOLS FOR DIRECT
MEASUREMENTS OF CONTACT ANGLES ON AGGREGATE AND
ASPHALT BINDER SURFACES USING A SESSILE DROP DEVICE

Major Field: CIVIL & ENVIRONMENTAL ENGINEERING

Abstract: Over the last several decades, the contact angle measurements have attained an increased popularity in several industries such as mining, petroleum, painting, coating, medicine, and recently in asphalt pavement materials. Contact angle measurement is a fundamental approach to determine the interfacial interaction that exists between a solid and a liquid, and between two different solids. In other words, one can calculate the surface free energy components of a solid material by using contact angle measurements.

Surface energy interactions between the asphalt binder and aggregate are known as the fundamental approaches to predicting the mechanisms in the moisture damage process in asphalt mixes. The moisture damage is simply known as the loss of bonding strength between asphalt binder and aggregate, and as well as within the binder itself in the presence of moisture. Therefore, it is important to know the surface energy parameters of these materials for realistic characterization of the moisture damage process in asphalt mixtures. The field of surface energy measurement and its application for moisture damage evaluation is very recent and in the developing stages. Wilhelmy Plate (WP) method and Universal Sorption Device (USD) are the two most widely used techniques for surface free energy measurements. The former is being used for asphalt binder and the latter is equipped for aggregates.

This thesis introduces a Sessile Drop (SD) device and new testing protocols for measuring the contact angles directly on asphalt binder and aggregate surfaces. Seven different aggregates and one asphalt binder from Oklahoma have been tested using the Sessile Drop method and the surface energy components of each material have been calculated using the Good-van Oss-Chaudhury (GVOC) approach and the measured contact angles. The calculated surface energy parameters have been compared with the same surface energy components of similar materials found in the literature. The comparison has indicated that both SD and WP methods have yielded similar results on asphalt binder specimens. However, the results from SD and USD methods on similar aggregate specimens are not in agreement and there are some significant differences.

TABLE OF CONTENTS

Chapter	Page
I. INTRODUCTION	1
1.1. Problem Statement	1
1.2. Objective of the Research Study	2
1.3. Organization of the Thesis	3
II. CONTACT ANGLE MEASUREMENTS	5
2.1. Sessile Drop Method	5
2.2. Universal Sorption Device	7
2.3. Wilhelmy Plate Method	8
2.4. Column Wicking and Thin Layer Wicking Methods	9
2.5. Heat of Immersion Method	10
III. SURFACE FREE ENERGY AND ITS COMPONENTS	11
3.1. Surface Energy Concept	11
3.1.1. Interfacial Lifshitz-van der Waals Interactions	12
3.1.2. Polar or Lewis Acid-Base Interactions	14
3.1.3. Young's Equation	16
3.2. Equilibrium Spreading Pressure	20
3.3. Adhesion and Cohesion	21
3.4. Wettability	23

Chapter	Page
IV. TESTING METHOD.....	25
4.1. Testing Protocol for Aggregates	25
4.1.1. Sample Preparation for Aggregates	26
4.1.2. Contact Angle Measurements on Aggregates	33
4.2. Testing Protocol for Asphalt Binder	35
4.2.1. Sample Preparation for Neat Asphalt Binder.....	35
4.2.2. Sample Preparation for Asphalt Binder with WMA Additives	38
4.2.3. Contact Angle Measurements on Asphalt Binder.....	39
V. TEST RESULTS.....	42
5.1. Contact Angle Data.....	43
5.2. Surface Energy Components.....	46
VI. DISCUSSIONS.....	50
VII. CONCLUSIONS	55
VIII. RECOMMENDATIONS	58
REFERENCES	59
APPENDICES	67

LIST OF TABLES

Table	Page
3-1 Surface energy components of three liquid probes used in this study.....	19
3-2 Varying contact angles and their corresponding interactions.....	24
5-1 Average contact angles and standard deviations of specimens using the Sessile Drop device.....	43
5-2 Average contact angles measured on PG 64-22 binder with different percentages of WMA additives using the Sessile Drop device	45
5-3 Surface free energy components of aggregates from contact angle measurements using the Sessile Drop method.....	48
5-4 Surface energy components of PG 64-22 neat binder and PG 64-22 binder with WMA additives.....	49
6-1 Surface free energy components of different geological materials in literature.....	52
6-2 Surface energy components of PG 64-22 neat binder compared to results in the literature	53
B-1 Final contact angle results with PG 64-22 neat binder	72
B-2 Final contact angle results on aggregate samples with Distilled Water.....	73
B-3 Final contact angle results on aggregate samples with Diiodomethane	74
B-4 Final contact angle results on aggregate samples with Ethylene Glycol.....	75
B-5 The Surface Free Energy components of all samples.....	76
B-6 Contact angle results on PG 64-22 neat binder with Distilled Water	77
B-7 Contact angle results on PG 64-22 neat binder with Diiodomethane.....	78
B-8 Contact angle results on PG 64-22 neat binder with Ethylene Glycol	79

LIST OF FIGURES

Figure	Page
2-1 Schematic drawing of the Sessile Drop device	5
2-2 The Sessile Drop device testing a flat aggregate specimen.....	6
2-3 Schematic illustration of the Universal Sorption Device	7
3-1 Schematic drawing of the contact angle between a liquid and a solid	17
3-2 An illustration of the surface tension.....	22
3-3 Adhesion between water and wood	23
4-1 Hillquist RF 20-24 slab saw	27
4-2 The polishing device.....	28
4-3 Silicon carbide grits	29
4-4 Application of silicon carbide grits on a specimen.....	30
4-5 Cleaning the sample with hexane	31
4-6 The desiccator with anhydrous calcium sulfate crystals	32
4-7 Davis limestone and Snyder granite specimens before the measurements	32
4-8 The placement of the solid specimen in the FTA 1000B	34
4-9 FTA 1000B capturing the images of a solid specimen to determine the contact angles	35
4-10 PG 64-22 Binder sample from Muskogee, Oklahoma	36
4-11 PG 64-22 Binder divided into a number of tin canisters and kept in the oven.....	37
4-12 PG 64-22 asphalt binder in small canisters and glass slide specimen	38
4-13 The FTA software processing a snapshot of the sessile drop on a solid specimen	41
5-1 Average contact angles of the specimens with three different probe liquids	44
5-2 Average contact angles of PG 64-22 binder with different percentages of WMA additives	46
A-1 IFT results before the calibration.....	68
A-2 The calibration window	69
A-3 IFT results after the calibration.....	70

CHAPTER I

INTRODUCTION

1.1. Problem Statement

According to the National Asphalt Pavement Association, the United States has more than 2.7 million miles of paved roads and 94% percent of the paved roads are surfaced with asphalt (U.S. Department of Transportation, 2008). The federal government invested \$58 billion in transportation improvements through the core federal transportation improvement programs during the fiscal year 2011 (American Road & Transportation Builders Association, 2012). The amount of money spent for these improvements can be minimized by selecting higher performing materials in terms of moisture damage prior to the construction stage.

The performance of asphalt pavement is closely related to adhesive bonding, which is the interaction energy and strength between asphalt binder and aggregate (Curtis et al., 1991). A good adhesion bonding is essential to ensure good performance of asphalt concrete, such as resistance to moisture damage and fatigue (Kanitpong and Bahia, 2005; Hefer et al., 2006; Masad et al., 2006; Lu and Harvey, 2008; Wasiuddin et al., 2008; Pinto et al., 2009).

The loss of strength and durability in asphalt mixtures due to the effects of moisture is referred as moisture damage (Masad et al., 2006; Bhasin and Little, 2007; Lu and Harvey, 2008). Moisture weakens the surface bonds between the asphalt binder and aggregate (Cheng et al., 2002). It is therefore very crucial to identify those binders and aggregates that can form a mix that is susceptible to moisture damage. In order to define the best binder-aggregate pair in terms of

moisture damage and adhesive/cohesive bonding, surface free energy analysis can be used (Bhasin and Little, 2007). The strength of the interface bonding is predictable when the wet adhesive bond strength (i.e., surface energy in wet condition) is compared with the dry adhesive bond strength (i.e., surface energy in dry condition) between the binder and aggregate (Lytton et al., 2005).

In these recent studies, the Wilhelmy Plate (WP) device was used to measure the surface energy components of asphalt binders and the Universal Sorption Device (USD) was employed to measure the surface energy components of aggregates. The WP method requires about three testing days for an operator to prepare a sample and run the test on one asphalt specimen, and it requires about ten days for an operator to prepare a sample and run the test on one aggregate specimen using the USD equipment. The preparation of uniform and neat samples for the WP method requires some skill and practice by the user, and for the USD test a skilled operator with appropriate training is required to conduct the test. The capital on these two devices is also high. A WP device costs more than \$30,000 and the USD costs about \$100,000. On the other hand, the Sessile Drop (SD) device is a simple equipment, which is relatively accurate, reliable, and economical for the measurement of surface energy components of asphalt binders and aggregates. The SD type devices have widely been used in different fields like mining, chemical, petroleum, geology, coating, painting, printing for direct measurement of contact angles (Fowkes, 1963; van Oss, 1994). The device can easily be setup in the laboratory with a relatively small capital (about \$20,000). The test procedure is very simple and requires minimal training.

1.2. Objective of the Research Study

This research study evaluates a sessile drop device (FTA 1000B series from Firsttenangstroms) on small core rock specimens and asphalt binder for measurement of contact angles and calculation of surface free energy components. New testing protocols for sample preparation and for using the sessile drop device are presented as part of the research study.

- Several aggregate specimens (Davis limestone, Snyder granite, Dolese Cooperton limestone, Hanson Davis rhyolite, Martin Marietta Mill Creek granite, Dolese Hartshorn limestone, and Pryor limestone) and one asphalt binder specimen (Muskogee, PG 64-22) from Oklahoma are tested for contact angle measurements using the sessile drop (SD) device.
- The results of the surface energy components from the SD contact angle measurements are compared to the results obtained on similar aggregate specimens and other geological materials in the literature using the SD, USD and Column Wicking methods.
- Similarly, the SD results on PG 64-22 asphalt binder are compared to the WP measurements on similar grade asphalt binder materials.

1.3. Organization of the Thesis

Chapter II presents a brief background on contact angle and surface energy measurement techniques and compares their advantages/disadvantages. The following methods are discussed in Chapter II:

- Sessile Drop (SD) Device,
- Universal Sorption Device (USD),
- Wilhelmy Plate (WP) Method,
- Column Wicking and Thin Layer Wicking Methods,
- Heat of Immersion Method.

Chapter III outlines theoretical background for surface free energy, Good - Van Oss – Chaudhury (GVOC) approach, adhesion-cohesion, wettability, and spreading pressure in calculation of surface free energy components.

Chapter IV introduces the sample preparation and testing protocols developed for the sessile drop device for direct measurements of contact angles on the surfaces of aggregate and asphalt binder specimens.

Chapter V presents the findings from the contact angle measurements with the sessile drop device and calculations of surface energy components using the contact angle data

Chapter VI contains discussion of the test results from the SD device and comparison of those findings with the results obtained using different methods on similar materials in the literature. The surface energy components of the materials used in this study are compared to the surface energy components of similar materials measured/calculated by different methods in the literature.

Chapter VII concludes this research study.

Chapter VIII includes the suggestions about future studies on this research subject.

CHAPTER II

CONTACT ANGLE MEASUREMENTS

2.1. Sessile Drop Method

Contact angle measurement, first described by Thomas Young in 1805, remains at present the most accurate method for determining the interaction energy between a liquid and a solid (van Oss, 2002). The Sessile Drop method is used to measure advancing contact angles of probe liquids with a solid surface and is suited for both asphalt binders and aggregates. Contact angles are measured directly by dispensing a drop of the probe liquid on the solid surface and capturing an image of the drop (van Oss, 1994). The captured image can be analyzed using a computer with image processing software to obtain the contact angle of the liquid at the edge of the drop (Figure 2.1).

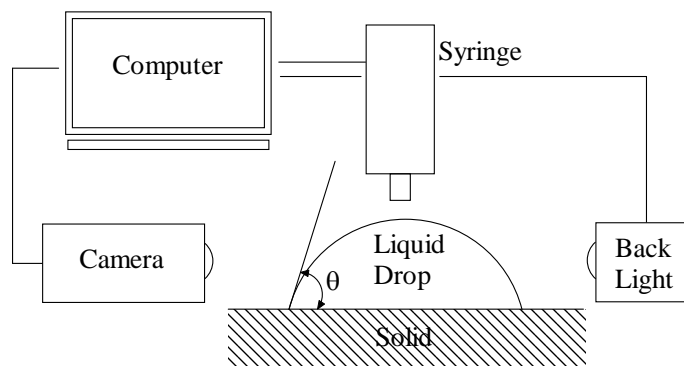


Figure 2-1 Schematic drawing of the Sessile Drop device

The sessile drop instrument (FTA 1000B Series from Firsttenangstroms) captures video images of liquid droplets and analyzes their shape and size to determine various surface chemistry quantities

such as contact angles, interfacial tension, pendant and sessile drop volumes, and spreading. The instrument is fully automated and can be controlled with the provided software on a computer. The device is fitted with a precise stepper motor drive syringe pump that can both push out and pull in fluid. In this way, advancing and receding contact angles can be measured over the sample surface. The fully automated single syringe dispenser can form drops of selected volume and automatically touch them off on samples for contact angle measurements. The advancing and receding contact angles can also be measured using the tilting plate mounted on the instrument. With the tilting plate frame, the instrument tilts up to a 90° angle. This device can be set up in the laboratory with a relatively small capital (about \$20,000). Figure 2.2 shows the instrument during testing a flat rock aggregate specimen.

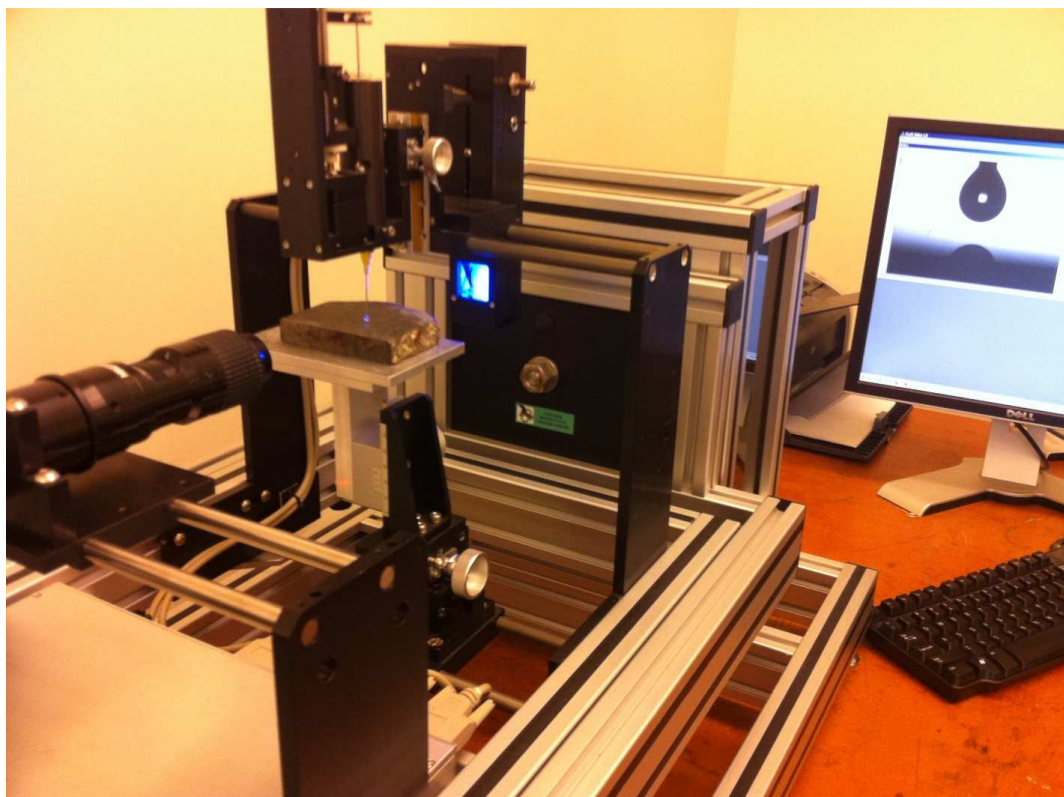


Figure 2-2 The Sessile Drop device testing a flat aggregate specimen

2.2. Universal Sorption Device

The Universal Sorption Device (USD) is usually employed to measure the surface free energy components of the aggregates *indirectly*. The gas adsorption characteristics of the probe liquids, whose surface energy components are known, are used to calculate the Surface Free Energy (SFE) components of the aggregates in USD method (Cheng, 2002).

Both USD and SD methods can employ the same probe liquids in the analysis. However, while the SD uses the probe liquid in the form of liquid drops, the USD uses them in the gas form. The probe liquids in the USD method are used to measure the spreading pressure with the aggregate while the probe liquids in the SD method are used to measure the contact angles directly.

The USD consists of a magnetic suspension balance system to measure the mass of the sample, a computer (software), temperature control unit, vacuum system and its regulator, pressure transducer, solvent container, and a vacuum desiccator (Cheng, 2002).

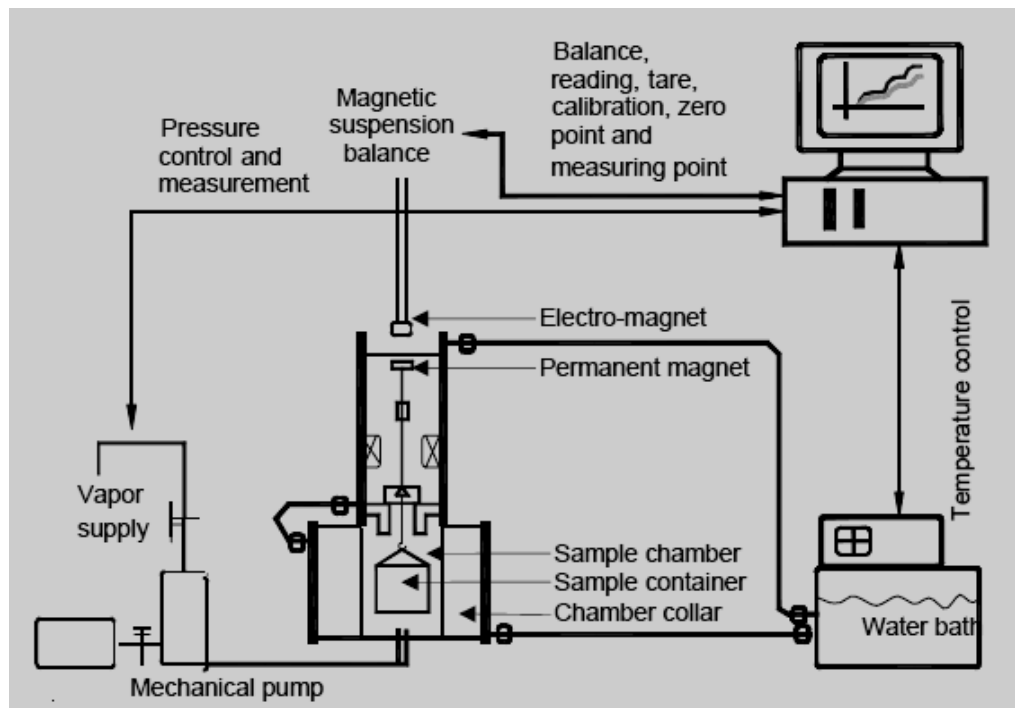


Figure 2-3 Schematic illustration of the Universal Sorption Device (Cheng 2002)

In order to use the USD on aggregates, the samples should be clean and degassed under high temperature. The samples are vacuumed in a sorption cell which is air-tight. Then, the USD takes the probe vapor into the sorption cell in small quantities. The increments of the probe vapor are increased gradually to reach different relative pressure levels. Once the adsorption isotherm is obtained, the equilibrium spreading pressure (π_e) of that particular probe vapor on the aggregate sample can be calculated. This process is repeated with different probe vapors until the equilibrium spreading pressures on the aggregate are obtained. Then, using the Good-van Oss-Chaudhury (GVOC) approach for the work of adhesion, the surface energy components of the aggregate are calculated (Bhasin, 2006; Cheng, 2002; van Oss et al., 1988; van Oss, 1994; Howson et al., 2007).

The testing protocol for the USD is very complicated and time consuming. According Cheng (2002), preparation and testing of an aggregate specimen take about 64 hours after the sieve analysis and washing the aggregates. On top of 64 hours, more time is spent during the testing of the aggregates with different probe vapors. Furthermore, each and every unit of the USD must be calibrated before each test. The weight of the sample and the temperature in chamber unit must be precise. A high level of expertise is required to use the USD and conduct laboratory experiments.

2.3. Wilhelmy Plate Method

Wilhelmy plate is a thin plate that is used to measure equilibrium surface or interfacial tension at an air–liquid or liquid–liquid interface. In this method, the plate is oriented perpendicular to the interface, and the force exerted on it is measured. Based on the work of Ludwig Wilhelmy, this method finds wide use in the preparation and monitoring of Langmuir–Blodgett films which consist of the material deposited from the surface of a liquid onto a solid substrate by immersing the solid into the liquid (Holmberg, 2002).

In addition to measuring the surface tensions, Wilhelmy plate method is also an alternative method for measuring the contact angles indirectly (Shang et al., 2008). In this method, a sensitive force meter is employed in order to measure a force that can be translated into a value of the contact angle. A small plate-shaped sample of the solid which is attached to the arm of a force meter is vertically dipped into the probe liquid, and the force exerted on the sample by the liquid is measured by the force meter.

In the Wilhelmy plate testing, a specimen of an appropriate size must be produced with a uniform cross section in the submersion direction, and the wetted length must be measured with precision. In addition, this method is only appropriate if both sides of the specimen are identical, otherwise the measured data will be a result of two completely different interactions (Rulison, 1996).

2.4. Column Wicking and Thin Layer Wicking Methods

The column wicking method is used to measure the contact angles on powdered or porous materials (van Oss, 1994). The contact angle is calculated after the speed of the capillary rise into the porous medium is measured. In order to obtain better results, the pore structure of the material must stay uniform during the capillary rise. On the other hand, the pore structure of the specimen changes for some colloids that are prone to shrink or swell (Shang et al., 2008).

This problem has been solved by the development of the thin-layer wicking method. In this method, a rigid thin layer is created by depositing the colloidal particles on a flat surface (van Oss et al., 1992). A large variety of minerals can be tested using these methods. According to Costanzo et al. (1995), thin-layer wicking method reveals almost identical contact angles compared to the sessile drop method on cubic hematite particles.

2.5. Heat of Immersion Method

The contact angles of powdered samples can also be measured by Heat of Immersion method (also known as Microcalorimetric method). In this technique, first the powder is degassed to remove the pre-adsorbed moisture. The sample is then immersed in the probe liquid (Groszek, 1962) for heat of immersion measurements. As the hydrophobicity of the sample increases, the heat of immersion in water decreases. The calculation of contact angles rely on rigorous thermodynamic relations (Yildirim, 2001). Once the contact angle values are determined from the heats of immersion of three different probe liquids, the SFE components are calculated using the GVOC theory.

CHAPTER III

SURFACE FREE ENERGY AND ITS COMPONENTS

3.1. Surface Energy Concept

The molecules in the bulk of a solid material are surrounded by the same type of molecules and thus have force balance. However, if the material is cut, the molecules on the surface become unbalanced and therefore have a certain amount of excess energy compared with the molecules in the bulk of the material. The surface energy may therefore be defined as the excess energy at the surface of a material compared to the energy in the bulk of the material.

As first described by Thomas Young in 1805 in the Philosophical Transactions of the Royal Society of London, it is the interaction between the forces of cohesion and the forces of adhesion which determines whether wetting (the spreading of a liquid over a solid surface) will occur. If complete wetting does not occur, then a bead of liquid will form with a contact angle which is a function of the surface energies of the system.

Surface energy is most commonly quantified using a contact angle goniometer (Shang et al., 2008; van Oss, 2002; Giese and van Oss, 2002). In this research study, FTA 1000B contact angle goniometer was used as a sessile drop device. Detailed information about the FTA 1000B goniometer and the testing protocol can be found in following chapters.

The theory of surface free energy has been developed in industrial surface science and chemical

engineering, and is used reliably in many areas of engineering disciplines, such as mining, pharmaceutical, petroleum, coating, painting, and printing industries (Good, 1992; Elphinstone, 1997). Recent studies show that surface free energy (SFE) characteristics of binders and aggregates can be used in a mechanics-based approach to quantify moisture damage potential of asphalt mixes (Lytton et al., 2005; Wasiuddin et al., 2008).

For a liquid, the surface tension (force per unit length) and the surface energy density are identical. Water has a surface energy density of 0.072 J/m^2 and a surface tension of 0.072 N/m . As for solids, surface tension is typically measured in dynes/cm (i.e., the force in dynes required to break a film of length 1 cm). It can also be stated as surface energy in ergs per square centimeter.

3.1.1. Interfacial Lifshitz-van der Waals interactions

The Gibbs free energy of cohesion (ΔG^c) of a liquid is the formation of a cohesive area of the union of two bodies of the same material under the vacuum condition (Good, 1966).

$$\Delta G^c = -2\gamma^{Total} \quad (3.1)$$

Equation 3.1 is also valid for solids where ΔG^c is the free energy of the solid to interact with liquids and γ^{Total} is the total surface energy of the solid material (Giese, 1996). Fowkes (1964) stated that the surface free energy of materials could be considered to be a sum of components resulting from each class of intermolecular interaction.

Using the Lifshitz approach for van der Waals interactions in condensed media, Chaudhury (1984) showed that the dispersion, induction and dipole contributions to the Lifshitz-van der Waals (or apolar) component of the surface tension, γ^{LW} , are additive.

In colloid and surface science, the interfacial tension (γ_{ij}) between two different materials i and j is one of the most important concepts since it is directly related to a quantitative expression for

the free energy of interparticle or intermolecular interactions in condensed phase systems (Girifalco and Good, 1957). The interfacial tension between a solid and a liquid material and between two solid materials is not feasible to determine directly (Girifalco and Good, 1957). Hence, the interfacial tension (γ_{ij}) between these materials must be determined using the surface tensions of each material individually (γ_i and γ_j).

According to the experimental works of Good and Girifalco (1957) and Fowkes (1964), if only dispersion interaction forces are available between two condensed phase materials, i.e. a solid and a liquid, the interfacial tension between them (γ_{ij}^{LW}) is given by the following equation:

$$\gamma_{ij}^{LW} = \left(\sqrt{\gamma_i^{LW}} + \sqrt{\gamma_j^{LW}} \right)^2 \quad (3.2)$$

Recalling Equation 3.1, the apolar component of the free energy of cohesion of material i, is:

$$\Delta G_i^{cLW} = -2\gamma_i^{LW} \quad (3.3)$$

The free energy of interaction between materials i and j in vacuum is related to the surface tensions of these materials by the Dupré equation (Giese and van Oss, 2002):

$$\Delta G_{ij}^{LW} = \gamma_{ij}^{LW} - \gamma_i^{LW} - \gamma_j^{LW} \quad (3.4)$$

Substituting Equation 3.2 into Equation 3.4 the following equation is obtained,

$$\Delta G_{ij}^{LW} = -2\sqrt{\gamma_i^{LW}\gamma_j^{LW}} \quad (3.5)$$

This equation states that the atoms at an interface are pulled by those in the neighboring phase. Since the Lifshitz-van der Waals forces are always available at the surface, Equation 3.5 also suggests that the energy of interaction is negative, i.e., the interaction energy between two purely polar condensed phases is always attractive (Lobato, 2004).

3.1.2. Polar or Lewis acid-base Interactions

Up to the middle 1980s, only van der Waals attractions and electrostatic repulsion forces were considered as acting forces between particle surfaces (Chaudhury, 1984). Van Oss et al. (1987) first applied Lifshitz theory to macroscopic scale interactions between material surfaces. The van Oss et al. (1987) study established for the first time a clear distinction between apolar, or Lifshitz – van der Waals (LW) and polar, or Lewis acid-base (AB) interactions. According to the van Oss et al. (1987) theory (or sometimes called the Good-van Oss-Chaudhury or acid-base theory), the total surface free energy of any material is divided into two components (assuming that the electrostatic component is negligible as compared to the LW and AB interactions) based on the type of the surface forces. These components are the non-polar component, also referred to as the LW or the dispersive component, and the Lewis acid-base component (AB) (van Oss et al., 1987):

$$\gamma = \gamma^{LW} + \gamma^{AB} \quad (3.6)$$

Where γ is the surface free energy of the solid material (i.e., aggregate or binder); γ^{LW} is the Lifshitz – van der Waals component; and γ^{AB} is the Lewis acid-base component. The acid-base component can further be divided into two subcomponents as the Lewis acid component (γ^+) and the Lewis base component (γ^-) (van Oss et al., 1987).

Chaudhury (1984) showed that the three, apolar, electrodynamic forces are simply additive, and should be treated as a single entity as the Lifshitz van der Waals (LW) interactions. After this development, it became possible to examine the polar (Lewis Acid-Base) properties of surfaces separate from the electrodynamic (Lifshitz van der Waals) apolar properties. Moreover, the polar concept has been extended to include all electron donating and electron accepting phenomena, as encompassed in the more general acid-base framework of Lewis (van Oss et al., 1988). To emphasize the (Lewis) acid-base character of the pair interactions, the designation AB has been used.

Fowkes (1987) demonstrated the presence and importance of acid-base interactions between two interacting surfaces. Fowkes (1987) determined the values of acid-base (W_{ij}^{AB}) and Lifshitz-van der Waals (W_{ij}^{LW}) components of work of adhesion for various acidic and basic liquids on polymer surfaces as a function of acidity or basicity of the polymer. He showed that the contribution of acid-base (or polar) component to the work of adhesion (W_{ij}^a) is strictly dependent on the acidity or basicity of the solid (polymer) of interest.

Based on Fowkes's acid-base interaction approach, van Oss et al. (1987) suggested that electron-acceptor (Lewis acid) and electron-donor (Lewis base) interactions are essentially asymmetrical meaning that of a given polar substance i, the electron-acceptor and the electron-donor parameters are usually quite different hence they must be described by two distinct parameters. Therefore, for the AB interactions, the free energy of interaction between two materials, i and j is defined as:

$$\Delta G_{ij}^{AB} = -2 \left(\sqrt{\gamma_i^+ \gamma_j^-} + \sqrt{\gamma_i^- \gamma_j^+} \right) \quad (3.7)$$

Where the electron donor parameter is designated as γ^- (basic component) and the electron acceptor parameter is designated as γ^+ (acidic component).

The polar (AB) free energy of cohesion of material is then defined as:

$$\Delta G_i^{AB} = -4\sqrt{\gamma_i^+ \gamma_i^-} \quad (3.8)$$

From Equation 3.1, the polar component of the surface tension of material i is then defined as:

$$\gamma_i^{AB} = 2\sqrt{\gamma_i^+ \gamma_i^-} \quad (3.9)$$

From Dupré Equation 3.4, which is applicable for any type of interaction, the following equation can be defined (Lobato, 2004):

$$\Delta G_{ij}^{AB} = \gamma_{ij}^{AB} - \gamma_i^{AB} - \gamma_j^{AB} \quad (3.10)$$

This equation, expresses the interfacial tension, γ_{ij}^{AB} , between substances i and j, is given as follows:

$$\gamma_{ij}^{AB} = \Delta G_{ij}^{AB} + \gamma_i^{AB} + \gamma_j^{AB} \quad (3.11)$$

Substituting the value for ΔG_{ij}^{AB} from Equation 3.8 and the values for γ_i^{AB} and γ_j^{AB} from Equation 3.10 gives (van Oss, 1994):

$$\gamma_{ij}^{AB} = 2 \left(\sqrt{\gamma_i^- \gamma_i^+} + \sqrt{\gamma_j^- \gamma_j^+} - \sqrt{\gamma_i^- \gamma_j^+} - \sqrt{\gamma_i^+ \gamma_j^-} \right) \quad (3.12)$$

This can also be written as:

$$\gamma_{ij}^{AB} = 2 \left(\sqrt{\gamma_i^+} - \sqrt{\gamma_j^+} \right) \left(\sqrt{\gamma_i^-} - \sqrt{\gamma_j^-} \right) \quad (3.13)$$

Equation 3.13 shows that γ_{ij}^{AB} is not restricted to positive values or zero, as is the case for γ_{ij}^{LW} .

Rather, γ_{ij}^{AB} will be negative when either one of the following conditions is satisfied (van Oss 1994):

$$\gamma_i^+ > \gamma_j^+ \quad \text{and} \quad \gamma_i^- < \gamma_j^- \quad (3.14)$$

or

$$\gamma_i^+ < \gamma_j^+ \quad \text{and} \quad \gamma_i^- > \gamma_j^- \quad (3.15)$$

The surface tension components approach by Fowkes (1963) can be applied to interfacial tensions as follows:

$$\gamma_{ij} = \gamma_{ij}^{LW} + \gamma_{ij}^{AB} \quad (3.16)$$

Finally, the total expression for the interfacial tension between two condensed phases can be rewritten as:

$$\gamma_{ij} = \gamma_i^{Total} + \gamma_j^{Total} - 2\sqrt{\gamma_i^{LW} \gamma_j^{LW}} - 2\sqrt{\gamma_i^+ \gamma_j^-} - 2\sqrt{\gamma_i^- \gamma_j^+} \quad (3.17)$$

3.1.3. Young's Equation

Thomas Young, in 1805, described the equilibrium (or the interaction energy) between a liquid drop and a solid material in terms of their individual surface forces (or energy) and the interaction

force between them as shown in Figure 3.1 and given in Equation 3.18 (van Oss 1994). Contact angle (θ) measurement as described by Young remains at present the most accurate method for determining the interaction energy (or the work of adhesion) between a liquid (L) and a solid (S) (van Oss 2002):

$$\gamma_L \cos \theta = \gamma_S - \gamma_{SL} \quad (3.18)$$

Where, γ_S is the surface energy of the solid; γ_L is the surface energy (or surface tension) of the liquid; and γ_{SL} is the interfacial tension (or energy) between the liquid and the solid.

The derivation of the Young's equation assumes that the solid surface is smooth, rigid and homogeneous. Also, it should not react both chemically and physically with the liquid that will be used for contact angle measurements (Lam et al., 2002).

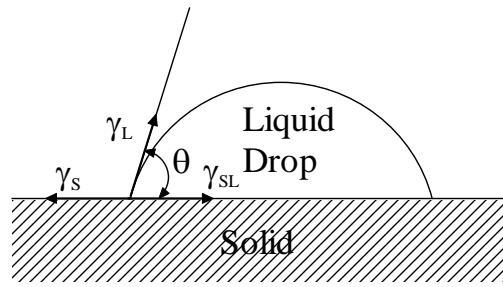


Figure 3-1 Schematic drawing of the contact angle between a liquid and a solid

In Equation 3.18, γ_L and $\cos \theta$ are known and γ_S and γ_{SL} are the unknown parameters. Using two different liquids gives rise to two equations with three unknowns. Thus, Equation 3.18, in the form given above is not practically usable. However, Dupre equation (Equation 3.19) along with Equation 3.18 can be used to determine contact angles (van Oss, 2002). Dupre equation represents the free energy of interaction between a solid and a liquid (Fowkes, 1963):

$$\Delta G_{SL} = \gamma_{SL} - \gamma_S - \gamma_L \quad (3.19)$$

Where, ΔG_{SL} represents the free energy of interaction between the solid and the liquid.

Combining Equation 3.18 and Equation 3.19 results in the Young-Dupre equation (Chaudhury 1984):

$$(1 + \cos\theta)\gamma_L = -\Delta G_{SL} \quad (3.20)$$

The total interaction energy consists of Lifshitz-van der Waals and Lewis acid-base interaction components (van Oss et al. 1987):

$$\Delta G_{SL} = \Delta G_{SL}^{LW} + \Delta G_{SL}^{AB} \quad (3.21)$$

In terms of individual surface energy components, Equation 3.21 takes the form (van Oss 2002):

$$\Delta G_{SL} = -2 \left(\sqrt{\gamma_S^{LW} \gamma_L^{LW}} + \sqrt{\gamma_S^+ \gamma_L^-} + \sqrt{\gamma_S^- \gamma_L^+} \right) \quad (3.22)$$

Where, γ_L^{LW} is the Lifshitz-van der Waals component of liquid; γ_S^{LW} is the Lifshitz-van der Waals component of solid; γ_L^+ is the Lewis acid component of liquid; γ_S^+ is the Lewis acid component of solid; γ_L^- is the Lewis base component of liquid; and γ_S^- is the Lewis base component of solid.

The combination of Equation 3.20 and Equation 3.22 gives the complete Young-Dupre equation that is widely used in determining the surface energy components of solid materials using contact angle measurements (van Oss 2002):

$$(1 + \cos\theta)\gamma_L = 2 \left[\sqrt{\gamma_S^{LW} \gamma_L^{LW}} + \sqrt{\gamma_S^+ \gamma_L^-} + \sqrt{\gamma_S^- \gamma_L^+} \right] \quad (3.23)$$

Equation 3.23 contains three unknowns (i.e., γ_S^{LW} , γ_S^+ , and γ_S^-). To obtain the unknown surface energy values for the solid (i.e., aggregate or binder) it is necessary to measure contact angles with three different liquid probes. Surface energy components of five most used probe liquids are given in Table 3.1. When selecting the appropriate combination of the three probe liquids, van Oss (2002) strongly recommend that two polar and one apolar probe liquids are selected. It is stated that two polar liquids must be significantly different with regard to their polarities. The calculated surface energy components will vary significantly with minor changes in contact angle measurements if the appropriate combination of the liquid probes is not selected (van Oss, 2002; Lytton et al., 2005; Bhasin, 2006). Based on the guidelines provided in van Oss (2002), diiodomethane (DIM) was used as the apolar liquid, while water and ethylene glycol were selected as polar liquids in this study.

Every material has a surface free energy from the fact that the molecules at the surface are subjected to unequal forces compared to their respective forces in the bulk material. It is not easy or rather not feasible to measure the surface components of the solid materials directly (van Oss, 2002). Therefore, the surface energy components of solid materials are usually determined indirectly using contact angle, vapor adsorption isotherm, or heat of immersion measurements. For the LW and AB interactions together, the method of choice is the determination of contact angles with drops of a small number of appropriate liquids deposited on a solid surface (Giese and van Oss, 2002). This method still remains the preferred approach, as it is the only method that allows the analysis of the surface properties of solid materials at their exact surfaces (not a few nanometers below the surface) (van Oss, 2002). This is particularly important because solid and liquid materials interact with one another through their exact surfaces (van Oss, 2002).

Table 3-1 Surface energy components of three liquid probes used in this study (ergs/cm² or mJ/m²) (van Oss, 2002).

Liquid Probe	γ^{Total}	γ^{LW}	γ^{AB}	γ^-	γ^+
	(ergs/cm ² or mJ/m ²)				
Water	72.80	21.80	51.00	25.50	25.50
Diiodomethane	50.80	50.80	0.00	0.00	0.00
Ethylene Glycol	48.00	29.00	19.00	1.92	47.00
Glycerol	64.00	34.00	30.00	57.40	3.92
Formamide	56.00	39.00	19.00	39.60	2.28

The universal sorption device (USD), Wilhelmy plate (WP) and the sessile drop (SD) methods make use of GVOC theory (Equation 3.23). The SD method measures the contact angles *directly* and adopts Equation 3.23 in its present form. The WP is based on kinetic force equilibrium and uses Equation 3.23 as well, but the contact angles are determined *indirectly*.

3.2. Equilibrium Spreading Pressure

While WP and SD methods make use of GVOC approach by utilizing Equation 3.23, the USD method introduces a spreading pressure to the left side of Equation 3.23 and drops the contact angle from the equation (Yildirim, 2001):

$$\pi_e + 2\gamma_L = 2 \left[\sqrt{\gamma_S^{LW} \gamma_L^{LW}} + \sqrt{\gamma_S^+ \gamma_L^-} + \sqrt{\gamma_S^- \gamma_L^+} \right] \quad (3.24)$$

Where the π_e is the spreading pressure determined from adsorption isotherms. However, the use of spreading pressure in the GVOC approach is still highly debated in the literature (van Oss 2002).

First introduced by Bangham and Razouk in 1937, some researchers in the field of colloid and surface science assumed that condensation of the probe liquid causes the complete wetting on the solid surface. The terms γ_{LV} and γ_{SV} representing the liquid-vapor and solid-vapor interfaces, respectively have been used in Young's force balance equation as:

$$\gamma_s = \gamma_{LV} \cos \theta + \gamma_{SL} + \pi_e \quad (3.25)$$

The equilibrium spreading pressure is represented as π_e , where $\pi_e = \gamma_s - \gamma_{SV}$.

This assumption might work with high energy surfaces. However, for low energy, homogeneous and smooth surfaces it cannot be applied. For contact angles larger than 10° , π_e is negligible (Wu 1982). Also, in the case of non-spreading liquids ($\gamma_L > \gamma_s$ and $\cos \theta < 1$), neither spreading nor pre-wetting occurs on low energy surfaces (van Oss 1994). Van Oss (2002) states that the acid-base theory is applicable with the current form of Equation 3.23 and may not be applicable to its derivative forms (Equation 3.24).

In this study, Young's equation is used without the spreading pressure term and the results of surface free energy (SFE) calculations are compared to the surface energies of similar materials found in the literature.

3.3. Adhesion and Cohesion

Adhesion and cohesion are two main components that affect surface tension. Molecules in liquid state experience strong intermolecular attractive forces. When those forces are between the same molecules, they are referred to as cohesive forces (i.e., molecules of a water droplet are held together by cohesive forces). Cohesive forces at the surface constitute surface tension. When the attractive forces are between different molecules, they are said to be adhesive forces (Adamson and Gast, 1997). The adhesive forces between water molecules and the walls of a glass tube are stronger than the cohesive forces leading to an upward turning meniscus at the walls of the vessel and contribute to capillary action (Hall and Hoff, 2002).

The cohesive forces between liquid molecules are responsible for the phenomenon known as surface tension. The molecules at the liquid surface are in a different state of energy equilibrium than the molecules below the surface (Figure 3.2). This condition forms a surface "film" which makes it more difficult to move an object through the surface than to move it when it is completely submersed (Petrucchi et al., 2007).

The cohesive forces between molecules down below a liquid surface are shared by all neighboring atoms. Those on the surface have no neighboring atoms above and exhibit stronger attractive forces upon their nearest neighbors on the surface. This enhancement of the intermolecular attractive forces at the surface is called surface tension (Figure 3.2) (Petrucchi et al., 2007).

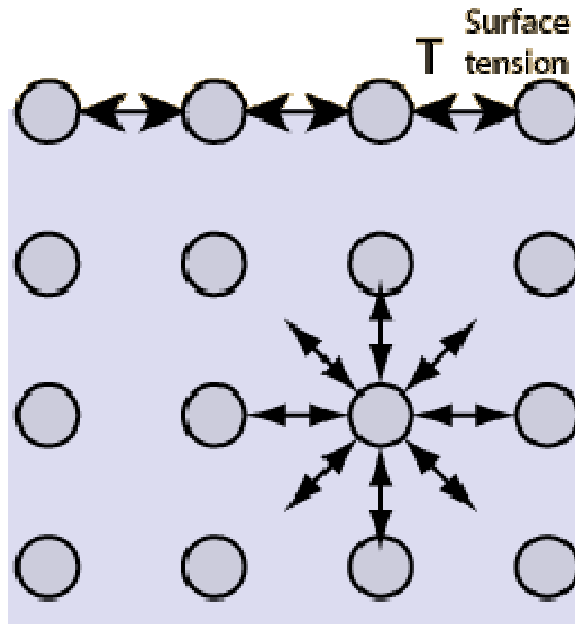


Figure 3-2 An illustration of the surface tension (<http://www.phy-astr.gsu.edu>)

Adhesion is the tendency of liquid molecules to create an attraction to a different substance (Figure 3.3). On the other hand, cohesion causes the liquid drop to create the minimum possible surface area which is a sphere under the influence of the gravitational force (Gugliotti, 2004). This is the lowest energy state for the liquid (Adamson and Gast, 1997; Gugliotti, 2004). On the other hand, adhesion causes the liquid drop to adhere to other substances.

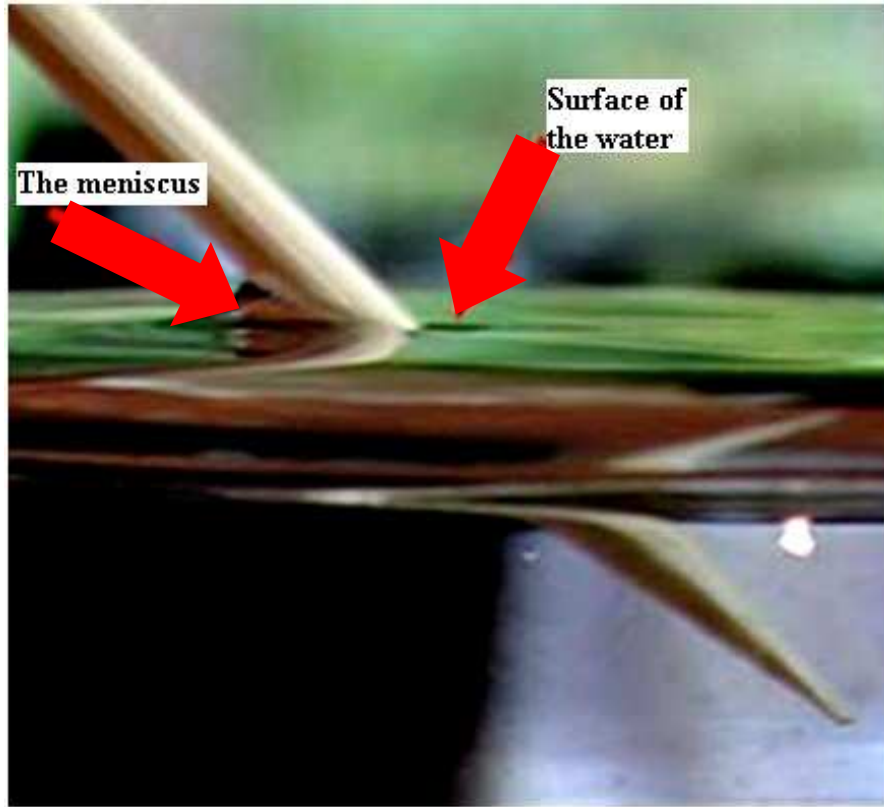


Figure 3-3 Adhesion between water and wood (<http://www.phy-astr.gsu.edu>)

3.4. Wettability

Wetting is the ability of a liquid to maintain contact with a solid surface, which is resulting from intermolecular interactions when the two materials are brought together in contact. The degree of wetting (also known as wettability) is determined by a force balance between adhesive and cohesive forces (Wasiuddin et al., 2008).

As explained before, an interface interaction between a liquid and a solid causes the liquid drop to spread across the surface. However, cohesive forces within the liquid cause the drop to form a spherical shape resisting against spreading. The contact angle (θ), as seen in Figure 3.1, is the angle at which the liquid–vapor interface meets the solid–liquid interface. The contact angle is determined by the resultant between adhesive and cohesive forces at equilibrium. As the tendency

of a drop to spread out over a flat, solid surface increases, the contact angle decreases. Thus, the contact angle provides an inverse measure of wettability (Sharfrin and Zisman, 1960).

A contact angle less than 90° (low contact angle) usually indicates that wetting of the surface is very favorable, and the fluid will spread over a large area of the surface. Contact angles greater than 90° (high contact angle) generally mean that wetting of the surface is unfavorable so the fluid will minimize the contact with the surface and form a compact liquid droplet (Sharfrin and Zisman, 1960).

When water is involved as the liquid, a wettable surface may also be termed hydrophilic and a non-wettable surface hydrophobic. Table 3.2 describes varying contact angles and their corresponding solid/liquid and liquid/liquid interactions (Eustathopoulos et al., 1999). For non-water liquids, the term lyophilic is used for low contact angle conditions and lyophobic is used when contact angles results are higher (Extrand, 2003).

Table 3-2 Varying contact angles and their corresponding interactions (Eustathopoulos et al., 1999).

Contact Angle ($^\circ$)	Degree of wetting	Strength of:	
		Solid/liquid interactions	Liquid/liquid interactions
$\theta = 0$	Perfect wetting	Strong	Weak
$0 < \theta < 90^\circ$	High wettability	Strong-weak	Strong-weak
$90^\circ \leq \theta < 180^\circ$	Low wettability	Weak	Strong
$\theta = 180^\circ$	Perfectly non-wetting	Weak	Strong

CHAPTER IV

TESTING METHOD

In this chapter, the sample preparation for aggregate and asphalt binder specimens and contact angle measurements with the Sessile Drop (SD) technique are discussed in detail. The testing protocol introduced below includes cutting, polishing, cleaning, and drying protocols for aggregates. The sample preparation for asphalt binder is very similar to the sample preparation technique used for the Wilhelmy Plate (WP) method.

The proposed testing protocol for the SD method has been developed stage by stage until the desired level of standard deviation (less than 3°), precision, and repeatability in contact angle measurements have been achieved.

4.1. Testing Protocol for Aggregates

As part of this thesis study, a testing protocol has been developed for the *direct* measurements of contact angles on aggregate specimens using the SD device. A number of different aggregate types (i.e., Davis Limestone, Snyder Granite, Dolese Cooperton Limestone, Hanson Davis Rhyolite, Martin Marietta Mill Creek Granite, and Pryor Stone-Pryor Limestone) were tested in this research study. All measurements on the aggregates were conducted with high purity probe liquids, namely; water, diiodomethane and ethylene glycol. The surface energy components of the probe liquids can be found in Table 3.1.

4.1.1. Sample Preparation for Aggregates

Large aggregate specimens (rocks) ranging in size from about 5 cm to about 20 cm in average diameter were obtained from different rock quarries in Oklahoma. Contact angle measurements can be conducted on small diameter (as small as 1 cm in diameter) specimens; however, it is more convenient to perform the tests on larger diameter specimens. The larger diameter specimens are easier to cut using a heavy duty diamond saw. In order to measure contact angles on the aggregate surfaces using the SD device, the aggregate surfaces must be relatively flat, smooth, and clean. It is therefore more practical to obtain flat surface aggregate specimens from relatively large size rocks. The development of the testing protocol for aggregate sample preparation of the SD method is given in detail in this section.

- The rocks were cut with thicknesses varying from about 1 cm to about 2 cm using mechanical diamond saws. The Covington Engineering Heavy Duty Slab Saw was employed for cutting smaller size rocks and the Hillquist RF 20-24 Slab Saw (Figure 4.1) was employed for obtaining larger size, flat rock surfaces.

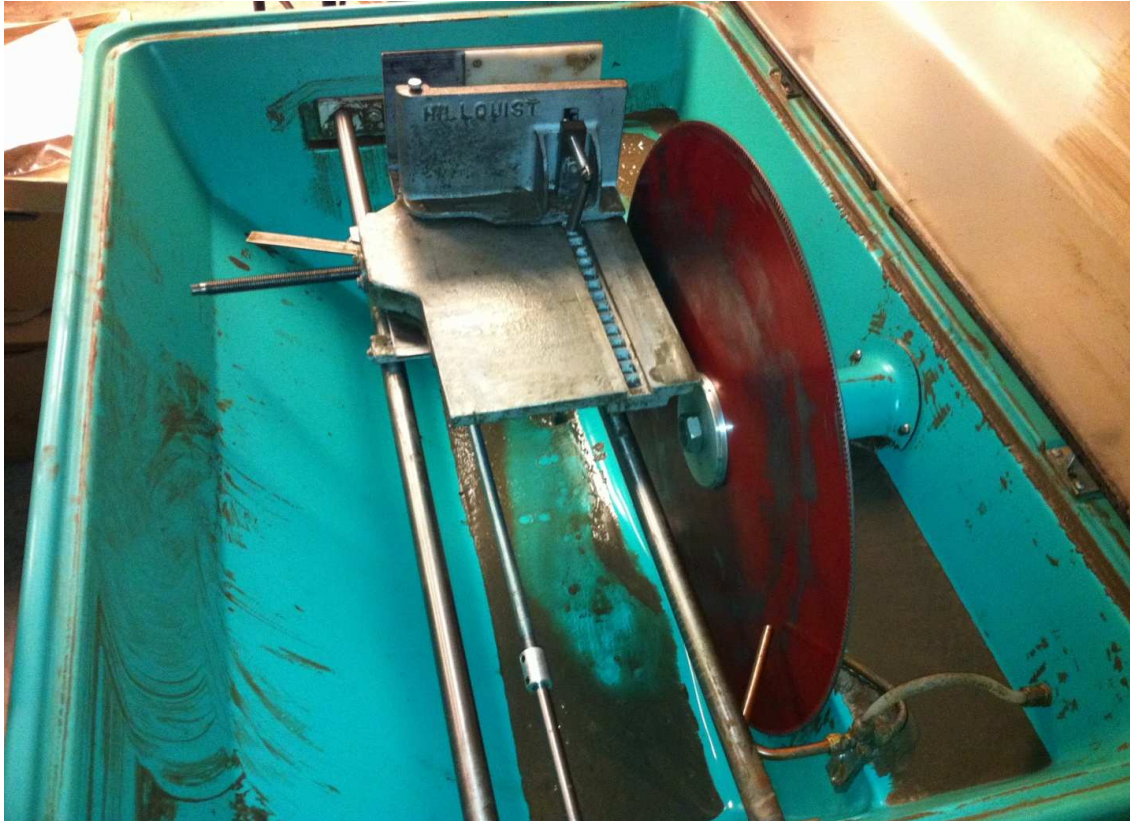


Figure 4-1 Hillquist RF 20-24 slab saw

Although the diamond saws have done a very good job in creating nice flat surfaces, there were still traces caused by the blades. To remove those traces and to reduce the amount of the roughness on the samples, a polishing test was undertaken using different grades of specific silicon carbide grit powders. The polishing device has a circular plate which basically spins with the silicon carbide powder mixed with the water on the plate (Figure 4.2).

- The flat surfaces of the rock specimens are held against the spinning plate for about 10 minutes.

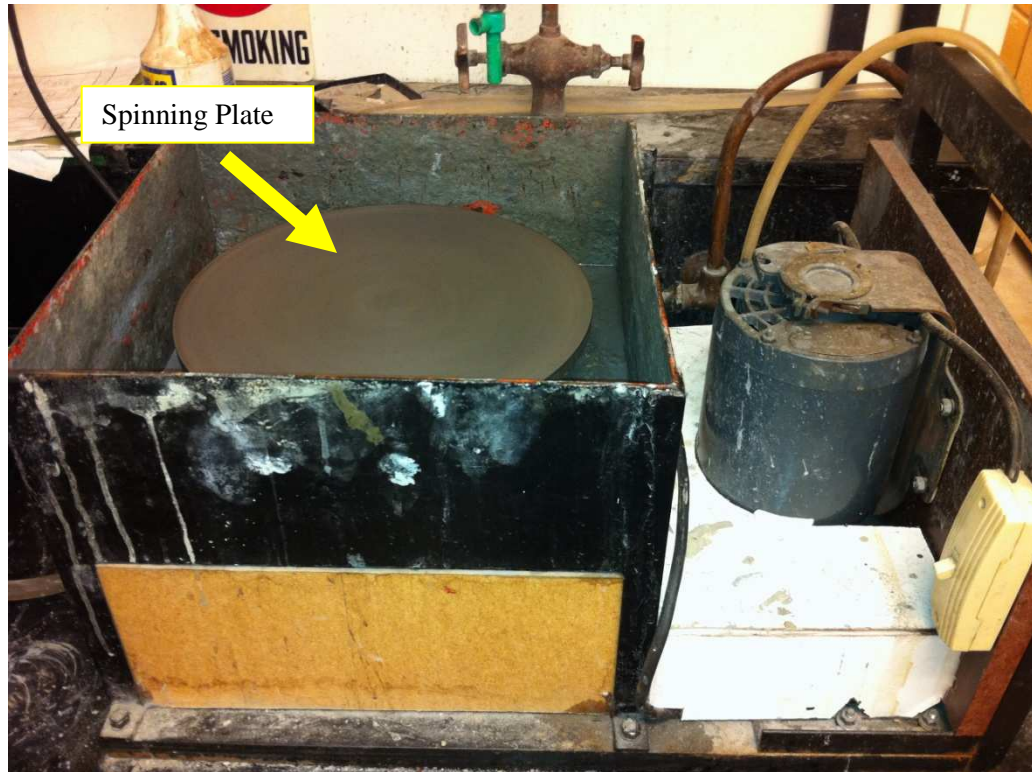


Figure 4-2 The polishing device

In order to achieve smoother surfaces, glass plates for specific silicon carbide grades were also used.

- In this stage of the polishing process, the silicon carbide grits were saturated with water on the glass plate surface until the mixture achieved the form of a paste. Then the aggregates were put onto the paste and moved around the surface of the glass with a uniform pressure applied by hand.
- Davis limestone and Snyder granite samples were polished using number 220 ($66\ \mu\text{m}$), 400 ($22.1\ \mu\text{m}$), 600 ($14.5\ \mu\text{m}$), and 1000 ($9.2\ \mu\text{m}$) grade silicon carbide grits (Figures 4.3 and 4.4).

The roughness of the sample surface plays a vital role in direct contact angle measurements.

Davis limestone and Snyder granite aggregates were polished using number 220 ($66\ \mu\text{m}$), 400 ($22.1\ \mu\text{m}$), 600 ($14.5\ \mu\text{m}$), and 1000 ($9.2\ \mu\text{m}$) grade silicon carbide grits. On the other hand,

Dolese Cooperton limestone, Hanson Davis rhyolite, Martin Marietta Mill Creek granite, Dolese Hartshorn limestone, and Pryor limestone aggregates were polished also with 5 micron aluminum oxide powder in addition to number 200, 400, 600, and 1000 grade silicon carbide grits. The 5 micron aluminum oxide powder has finer particle size, and reduces the surface roughness further. This change has made a considerable difference in repeatability, precision, and standard deviation of contact angle measurements. All the test results can be found in the next chapter.



Figure 4-3 Silicon carbide grits

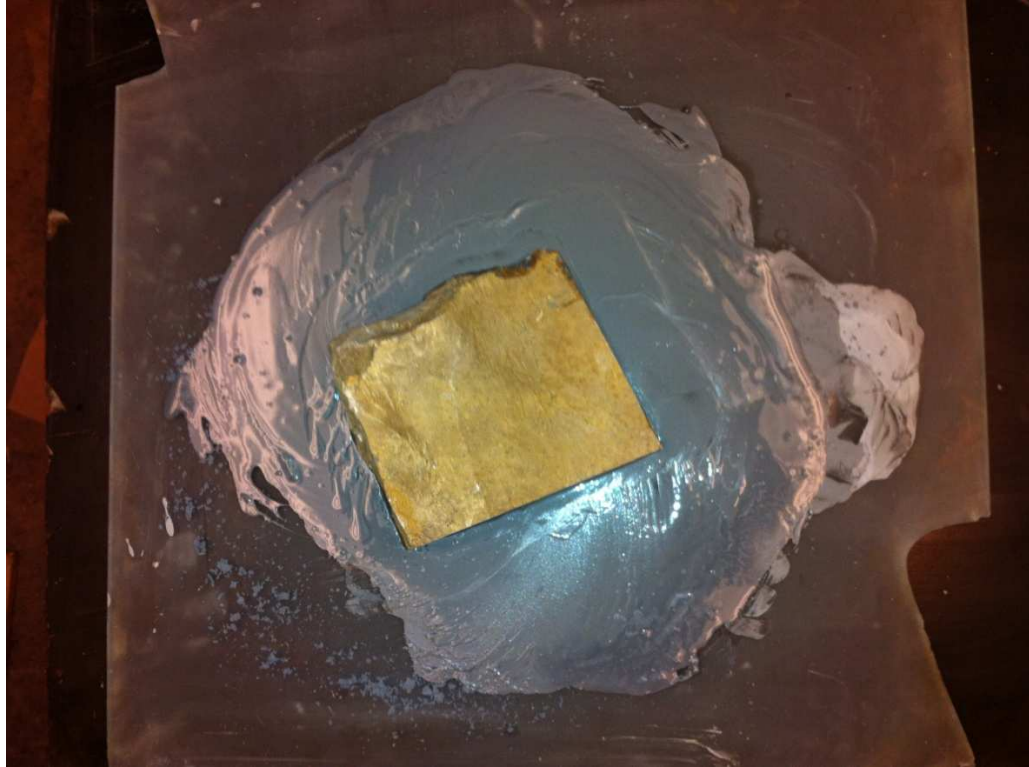


Figure 4-4 Application of silicon carbide grits on a specimen

During the cutting and polishing processes, the aggregates are usually contaminated with oil and grit powder material. Since oil and soap can change the cohesive and adhesive properties of solids (i.e., aggregates), any change in the surface properties of the materials will change the surface tension and contact angles directly. For this reason, a cleaning protocol was applied as follows.

- In order to remove the oil and grit powder material from the surface of the aggregates, the samples were washed thoroughly with soap and warm distilled water (Wilber, Personal Communication, 2011).
- The flat rock specimens then were cleaned using hexane. Paper towels were put in a pan and saturated with hexane (Figure 4.5). Both surfaces of each flat rock specimens were rubbed by wet paper towels to remove the residues of the oil used in the diamond saw cutting process (Wilber, Personal Communication, 2011).



Figure 4-5 Cleaning the sample with hexane

Contact angle measurements must be performed on relatively dry specimens for representative measurements without the interferences of moisture on the results.

- After the cleaning process, the rock specimens were put inside an oven at $105\pm 5^{\circ}\text{C}$ for 12 hours for drying.
- The samples were then allowed to cool down to room temperature in a desiccator with anhydrous calcium sulfate crystals (Figure 4.6).



Figure 4-6 The desiccator with anhydrous calcium sulfate crystals

Figure 4.7 depicts two aggregates that are prepared using the sample preparation protocol mentioned above and ready for testing for contact angle measurements using the SD device.



Figure 4-7 Davis limestone and Snyder granite specimens for contact angle measurements

4.1.2. Contact Angle Measurements on Aggregates

Once the sample preparation of aggregates is completed as given in the preceding section, the contact angles of the samples with three different probe liquids (water, diiodomethane, ethylene glycol) are determined using the Sessile Drop device. The following process is followed in multiple sets for each sample with each probe liquid until the desired repeatability and standard deviation are achieved. To avoid the contamination of the syringe in the SD device (Figure 4.8) with the different probe liquids, each probe liquid is dedicated with one syringe.

- The syringe that contains the probe liquid is refilled before the test. If a different probe liquid is going to be used, the syringe should also be replaced.
- The SD device is calibrated before each testing set (see Appendix A).
- Once the device is calibrated and the samples are at the testing temperature (at room temperature), the specimen is taken out of the desiccator and placed under the needle on the sample stage as shown in Figure 4.8. The SD device is equipped with an automated pump system to dispense a small amount of liquid on the specimen using the syringe.

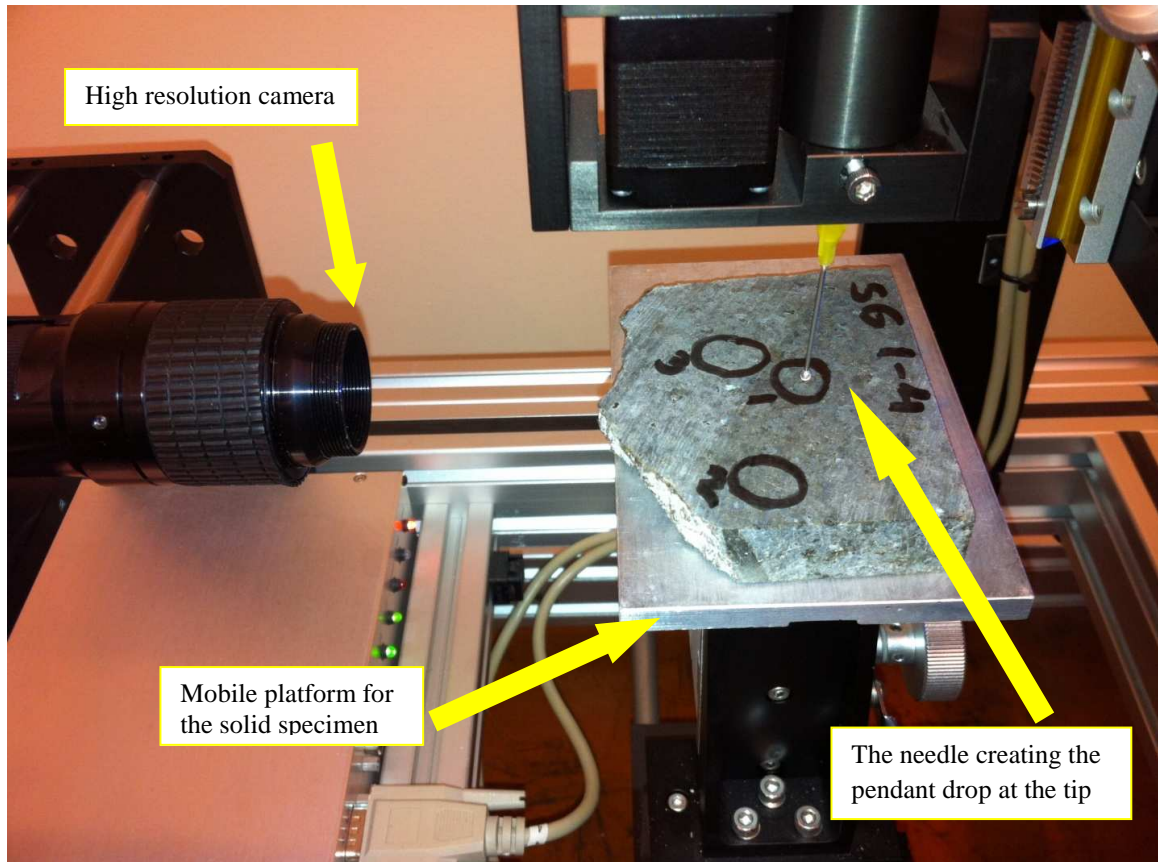


Figure 4-8 The placement of the solid specimen in the FTA 1000B

- About 10-15 μL of probe liquid is dispensed from the needle using the FTA software in the SD device computer system.
- While the liquid is still in the form of a pendant drop and at its full volume, the platform that holds the specimen is elevated slowly until the specimen touches the drop.
- The drop detaches from the needle and forms the sessile drop on the flat surface of the specimen.
- The high resolution camera constantly captures the images of the liquid-solid interface and sends it to the software for processing. The number of the images per second and test duration can be adjusted from the software. In this study, three images per second are used. The time period for a single test was 45 seconds.

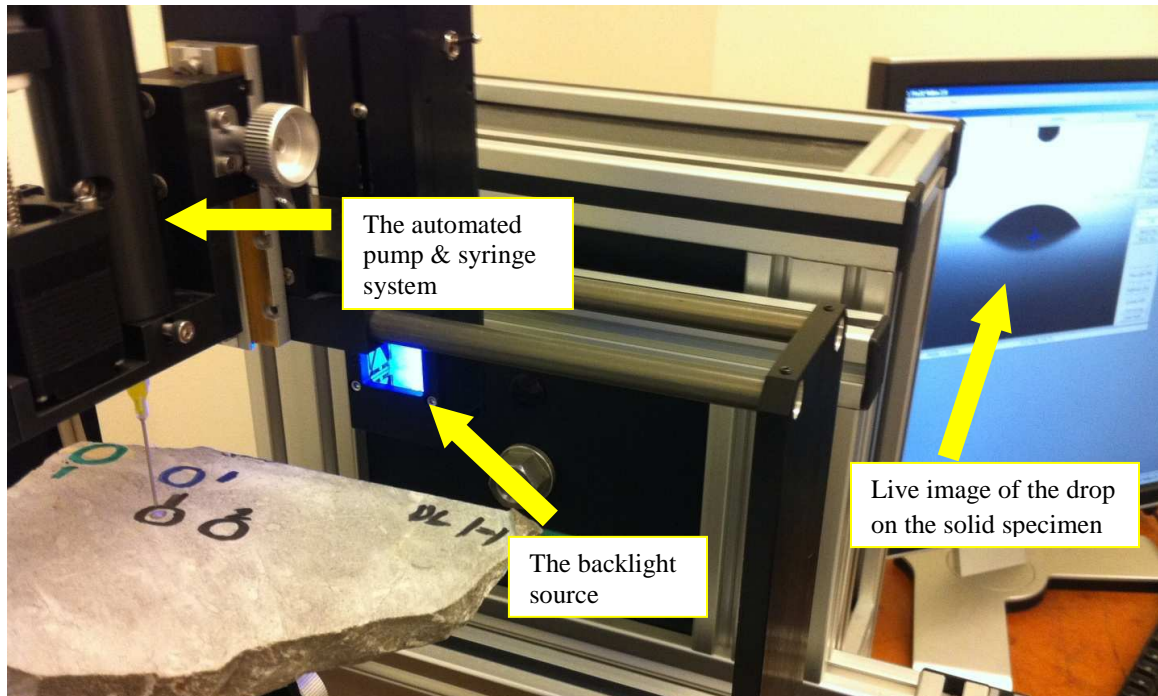


Figure 4-9 FTA 1000B capturing the images of a solid specimen to determine the contact angles

- Finally, the software processes each image and determines the average contact angles.
- The whole process is repeated for the second and third probe liquids.

4.2. Testing Protocol for Asphalt Binder

In this study, PG 64-22 asphalt binder has been used. The sample preparation and testing protocols for the neat asphalt binder specimens with and without Warm Mix Asphalt (WMA) additives (Sasobit®, Permatrac Plus®, and Evothrm®) are given below.

4.2.1. Sample Preparation for Neat Asphalt Binder

Sample preparation protocol for asphalt binder for the Sessile Drop (SD) method is very similar to the sample preparation protocol for the Wilhelmy Plate (WP) method. However, SD method has a clear advantage over WP. The SD device measures the contact angles *directly* while the WP measurements are based on the force equilibrium, and thus the contact angles are inferred

indirectly. A detailed testing protocol for asphalt binders using the Wilhelmy plate can be found in Lytton et al. (2005).

The sample preparation process of asphalt binder for the SD device is as follows.

- For specimen preparation, the bulk asphalt binder sample is heated in the oven at $105\pm 5^{\circ}\text{C}$ for one hour.



Figure 4-10 PG 64-22 Binder sample from Muskogee, Oklahoma

- After gaining some viscosity, the whole bulk material is divided into number of small canisters (Figure 4.11). The sample is divided into a number of canisters for maintaining the same level of aging for each consequent contact angle measurements using the sessile drop device.



Figure 4-11 PG 64-22 Binder divided into a number of tin canisters and kept in the oven

- Before each contact angle measurement, a canister with the binder inside is put into the oven at $105 \pm 5^\circ\text{C}$ for a period of one hour.
- After heating the binder, a plain microscopic glass slide with 76 mm x 25 mm x 1 mm dimensions is dipped into the melted binder for a few seconds and then held out of the canister for another a few seconds to let the excessive binder drop off the glass (Figure 4.12). This process is repeated a few times, if necessary, to obtain a flat and smooth surface area of the binder on the glass surface.
- The specimen is then allowed to cool down to room temperature in a desiccator with anhydrous calcium sulfate crystals overnight.
- Contact angle measurements can be conducted after the specimens have equilibrated to the testing (room) temperature.



Figure 4-12 PG 64-22 asphalt binder in small canisters and glass slide specimen

4.2.2. Sample Preparation for Asphalt Binder with WMA Additives

Contact angle measurements can also be performed on the binder samples mixed with the warm mix asphalt (WMA) additives using the SD device. Three WMA additives (Sasobit®, Permatac Plus®, and Evotherm®) with different percentages (0.5%, 1.0%, and 1.5%) were used in this study. The sample preparation protocol for binder with WMA additives is nearly the same as the sample preparation for the neat binder.

- For specimen preparation, the bulk asphalt binder sample is heated in the oven at $105 \pm 5^\circ\text{C}$ for one hour.
- After gaining some viscosity, the whole bulk material is divided into number of small canisters.
- The sample is divided into a number of canisters for maintaining the same level of aging process for each consequent contact angle measurements using the sessile drop device.
- Using a balance, the weights of the neat binder and the additive are measured for the desired mixture percentages (by weight).

- Each sample is kept in a different canister.
- Before each contact angle measurement, a canister with the binder inside is put into the oven at $105\pm 5^{\circ}\text{C}$ for one hour, stirring occasionally for homogeneous distribution of the WMA additive in the mixture.
- After heating the binder, a plain microscopic glass slide with 76 mm x 25 mm x 1 mm dimensions is dipped into the melted binder for a few seconds and then held out of the canister for a few more seconds to let the excessive binder drop off the glass slide. This process is repeated a few times, if necessary, to obtain a flat and smooth surface area of the binder on the glass slide surface.
- The specimen is then allowed to cool down to room temperature in a desiccator with anhydrous calcium sulfate crystals overnight.
- Contact angle measurements can be conducted after the specimens have equilibrated to the testing (room) temperature.

4.2.3. Contact Angle Measurements on Asphalt Binder

In this research study, contact angle measurements on the PG 64-22 binder from Ergon, Muskogee, Oklahoma were conducted using the SD method. For each probe liquid measurements, three glass slides were prepared. In total, six measurements were conducted for every probe liquid (two measurements on each slide). The glass slides were disposed after two measurements with the same probe liquid. This process was repeated for all three probe liquids. The contact angle measurements of the binder samples are conducted with three different probe liquids (Water, Diiodomethane, Ethylene Glycol) using the SD device. The following process is followed in multiple sets for each sample with each probe liquid.

- The SD device is calibrated before each testing set (see Appendix A).
- The syringe that contains the probe liquid is refilled before the test. If a different probe liquid is going to be used, the syringe should also be replaced or cleaned thoroughly.

- Once the device is calibrated and the samples are at the testing temperature (at room temperature), the specimen is taken out of the desiccator and placed under the needle attached to the syringe in the automated pump system of the SD device.
- About 10-15 μL of probe liquid is dispensed from the needle using the FTA software in the SD device system.
- While the liquid is still in the form of a pendant drop, the platform that holds the specimen is elevated slowly until the specimen touches the drop.
- The drop detaches from the needle and forms the sessile drop on the flat surface of the specimen.
- The high resolution camera constantly captures the images of the liquid-solid interface and sends it to the software for processing. The number of the images per second and test duration, if needed, can be adjusted from the software. In this study, three images per second were used. The time period for a single test was 45 seconds.

Finally, the software processes each image and determines the average contact angles.

The protocols for contact angle measurements on neat and modified asphalt binder specimens are the same.

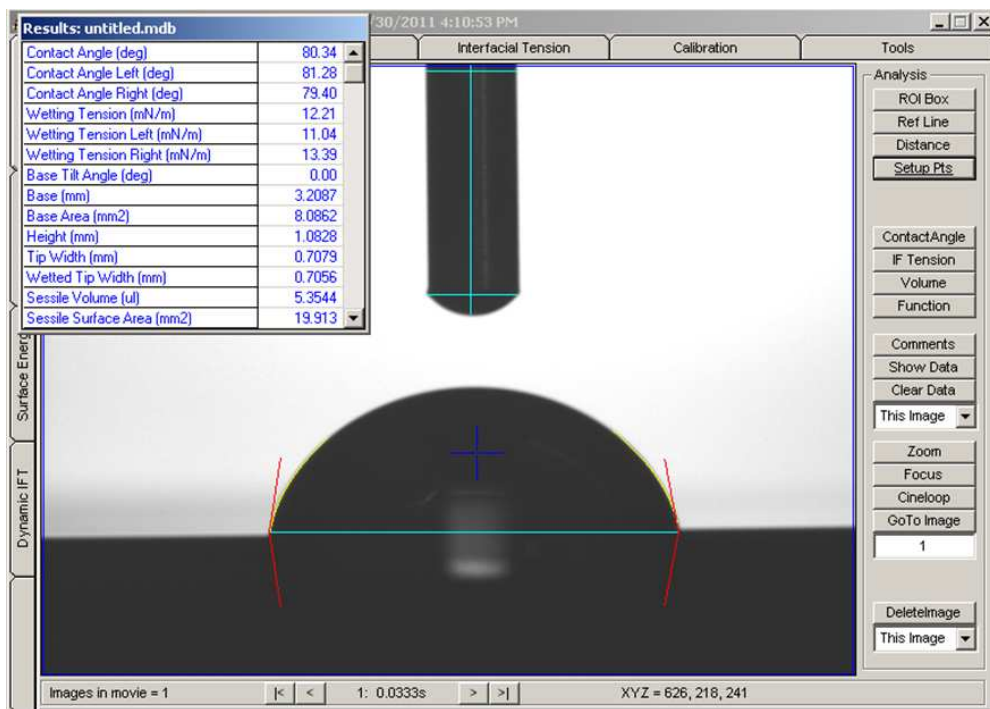


Figure 4-13 The FTA software processing a snapshot of the sessile drop on a solid specimen

CHAPTER V

TEST RESULTS

Contact angles of aggregates and asphalt binders were measured using the Sessile Drop (SD) device with three different probe liquids (Water, Diiodomethane, and Ethylene Glycol). The sample preparation and contact angle measurements of aggregates and asphalt binder were conducted according to the testing protocols given in Chapter IV. Contact angle measurements were performed on seven different aggregates (Davis limestone, Snyder granite, Dolese Cooperton limestone, Hanson Davis rhyolite, Martin Marietta Mill Creek granite, Dolese Hartshorn limestone, Pryor limestone) obtained from different rock quarries in Oklahoma and one binder (PG 64-22) from Ergon, Muskogee, Oklahoma. The PG 64-22 binder with different percentages of Warm Mix Asphalt (WMA) additives (Sasobit®, Permatac Plus®, and Evotharm®) were also tested for contact angle measurements using the SD device following the testing protocol given in Chapter IV.

The average contact angle values of ten measurements for each aggregate specimen and the average contact angle values of six measurements for each asphalt binder specimen can be found in this chapter. The average contact angles and corresponding standard deviations of each aggregate and neat binder specimens are given in Table 5.1.

Table 5.2 presents the average contact angles of PG 64-22 asphalt binder with different percentages of WMA additives. All the raw data are provided in Appendix B.

5.1. Contact Angle Data

The contact angle measurements on Davis Limestone and Snyder Granite were conducted in three sets and each set involved ten measurements. The average values of all the measurements are given in Table 5.1. The raw data is included in Appendix B. Direct contact angle measurements on all samples using the Sessile Drop (SD) device were performed using the sample preparation and testing protocols given in the previous chapter.

Table 5-1 Average contact angles and standard deviations of specimens using the Sessile Drop device.

Sample	Ethylene Glycol		Water		Diiodomethane	
	Average	S.D.	Average	S.D.	Average	S.D.
	(in degrees)					
Davis Limestone	61.7	2.2	79.4	4.7	46.4	1.5
Snyder Granite	58.6	3.9	74.6	4.0	49.8	3.8
Dolese Cooperton Limestone	43.8	2.6	65.7	1.9	41.7	1.0
Hanson Davis Rhyolite	33.2	1.0	60.9	1.2	45.0	0.8
Martin Marietta Mill Creek Granite	33.2	1.0	44.9	0.4	41.8	0.9
Dolese Hartshorn Limestone	31.3	2.5	64.2	2.0	42.8	2.3
Pryor Stone – Pryor Limestone	18.7	1.5	60.6	0.6	34.7	2.6
PG 64-22 Neat Binder	70.5	2.5	93.0	1.1	48.0	1.4

As it can be seen in Table 5.1, the standard deviations for Davis limestone and Snyder granite are comparably larger than the standard deviations of other aggregates (Dolese Cooperton limestone, Hanson Davis rhyolite, Martin Marietta Mill Creek granite, Dolese Hartshorn limestone, Pryor

limestone). The reason for this difference can be explained by the surface roughness levels of the samples from different polishing stages. As explained in Chapter IV, Snyder granite and Davis limestone specimens were polished using the 1000 grade (9.2 μm) silicon carbide grits while the other aggregate samples were polished further using the 5 micron aluminum oxide powder. Since these samples were polished using a finer grade powder, they had smoother surfaces compared to Snyder granite and Davis limestone. In the SD method the roughness of the solid surface plays a vital role in obtaining uniform and representative contact angle measurements. Hence it can be stated that higher levels of surface roughness of Snyder granite and Davis limestone samples caused higher standard deviations.

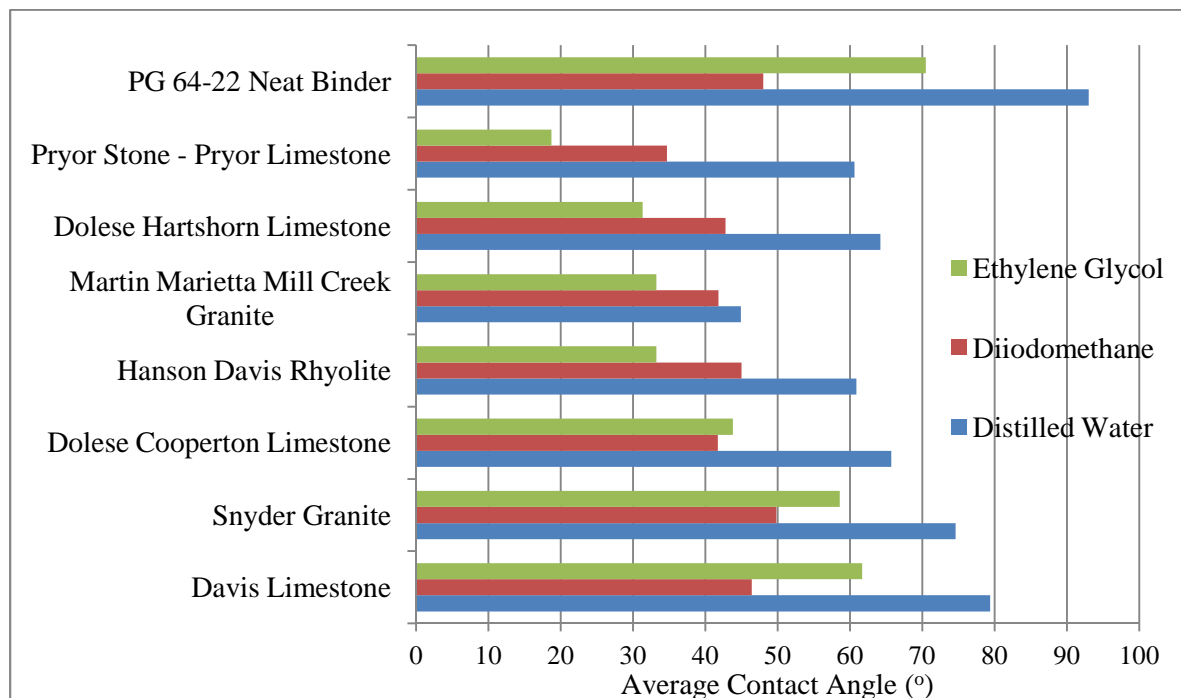


Figure 5-1 Average contact angles of the specimens with three different probe liquids

Contact angle measurements with distilled water on aggregate and binder specimens returned largest contact angle values compared to the other probe liquids. The reason for this behavior might be related to the interfacial tensions (IFT) of the probe liquids. The IFT of Diiodomethane and Ethylene Glycol (Table 3.1) are very close in magnitude and lower than the IFT of Distilled

Water. The exact relation was observed in the magnitudes of their contact angles (Table 5.1) on different aggregate surface. As far as the contact angle results on aggregates concerned, it was also observed that as the IFT decreased, the standard deviation of contact angles decreased as well.

Table 5-1 Average contact angles measured on PG 64-22 binder with different percentages of WMA additives using the Sessile Drop device.

WMA Additive	Water	Diiodomethane	Ethylene Glycol
Percentage	(Average Contact Angle Values in Degrees)		
Sasobit 0.5%	92.5	48.0	71.0
Sasobit 1.0%	90.0	46.5	69.5
Sasobit 1.5%	89.0	44.0	67.0
Evotharm 0.5%	90.0	48.0	70.0
Evotharm 1.0%	88.5	46.5	68.0
Evotharm 1.5%	85.0	45.5	68.5
Permatac Plus 0.5%	91.0	45.0	69.0
Permatac Plus 1.0%	89.5	42.5	68.5
Permatac Plus 1.5%	88.0	42.0	67.0

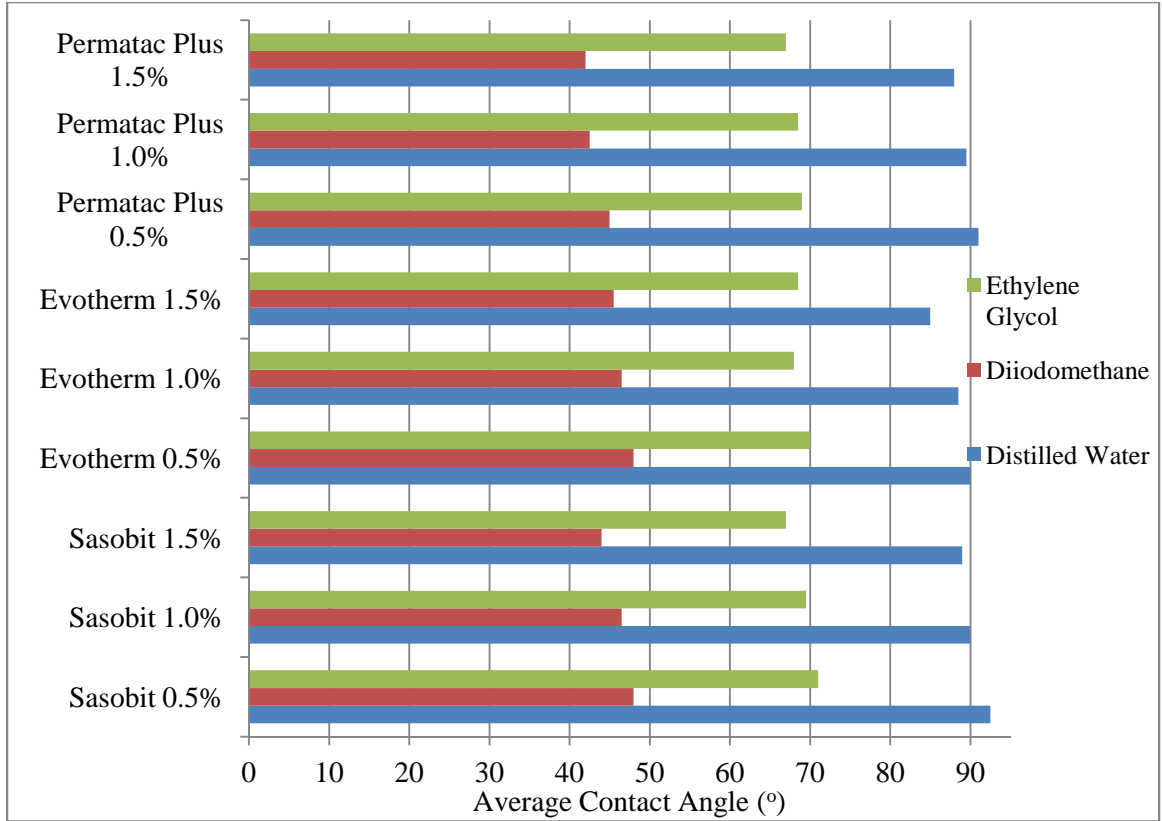


Figure 5-2 Average contact angles of PG 64-22 binder with different percentages of WMA additives

5.2. Surface Energy Components

The surface energy components of aggregates and asphalt binder evaluated in this study have been calculated using the Good - van Oss - Chaudhury (GVOC) approach (as given in Equation 3.23 in Chapter III). Equation 3.23 consists of four known surface energy components of the probe liquid (i.e., γ_L , γ_L^- , γ_L^+ , and γ_L^{LW} as listed in Table 3.1), and three unknown surface energy components of the solid (i.e., γ_S^- , γ_S^+ , and γ_S^{LW}), and a contact angle (θ) term. Equation 3.23 summarizing the GVOC approach is re-listed below:

$$(1 + \cos\theta)\gamma_L = 2 \left[\sqrt{\gamma_S^{LW}\gamma_L^{LW}} + \sqrt{\gamma_S^+\gamma_L^-} + \sqrt{\gamma_S^-\gamma_L^+} \right] \quad (3.47)$$

The unknown contact angle (θ) term is measured by the Sessile Drop (SD) device. The surface energy components of probe liquids can be found in the literature (Table 3.1). In order to solve Equation 3.23 for three unknown surface energy components of the solid (aggregate or binder in this case), the SD tests are conducted with three different probe liquids resulting in three equations with three unknowns. The average values of the contact angle measurements are implemented into Equation 3.23 with corresponding surface energy components of the probe liquids. Combining these three sets of equations, Equation 3.23 becomes a simple three equation-three unknown system which can be solved easily. The surface energy components of solids in this study have been calculated using a spreadsheet.

Table 5.3 and Table 5.4 depict the surface energy components of the aggregates and asphalt binder, respectively, from Oklahoma in the research study. The results of surface energy calculations in this study were compared to the surface energy components of various materials in the literature in the next chapter.

Table 5-2 Surface free energy components of aggregates from contact angle measurements using the Sessile Drop method.

Sample	γ^-	γ^+	γ^{AB}	γ^{LW}	γ^{Total}
	(ergs/cm ² or mJ/m ²)				
Davis Limestone	10.12	0.05	1.35	36.26	37.61
Snyder Granite	13.97	0.01	0.28	34.39	34.66
Dolese Cooperton Limestone	16.90	0.09	2.53	38.74	41.27
Hanson Davis Rhyolite	18.52	0.61	6.73	37.01	43.74
Martin Marietta Mill Creek Granite	39.45	0.08	3.45	38.69	42.14
Dolese Hartshorn Limestone	14.06	0.78	6.61	38.17	44.78
Pryor Stone – Pryor Limestone	14.37	0.90	7.20	42.17	49.37

Table 5-3 Surface energy components of PG 64-22 neat binder and PG 64-22 binder with WMA additives.

Asphalt Binder	γ^-	γ^+	γ^{AB}	γ^{LW}	γ^{Total}
	(ergs/cm ² or mJ/m ²)				
PG 64-22 Neat Binder	2.82	0.12	1.15	35.38	36.53
Sasobit 0.5%	3.22	0.16	1.42	35.38	36.80
Sasobit 1.0%	4.28	0.17	1.73	36.20	37.93
Sasobit 1.5%	4.12	0.13	1.44	37.54	38.98
Evothrm 0.5%	4.48	0.16	1.70	35.38	37.08
Evothrm 1.0%	4.83	0.13	1.57	36.20	37.78
Evothrm 1.5%	7.70	0.29	2.99	36.74	39.73
Permatac Plus 0.5%	3.47	0.16	1.49	37.01	38.50
Permatac Plus 1.0%	4.19	0.24	2.02	38.33	40.35
Permatac Plus 1.5%	4.72	0.20	1.95	38.59	40.54

Table 5.3 and 5.4 show that Lewis-Acid (γ^+) components are almost negligible compared to the Lewis-Base (γ^-) components as it was expected according to the GVOC approach (van Oss, 2002). Using the SD method Bargir et al. (2009) has measured the contact angles of various solid materials (stainless steel, gold, aluminum, etc.) and calculated their SFE components. The results showed that the values of γ^+ components of all materials were ranging from 0.01 ergs/cm² to 1.07 ergs/cm² (Bargir et al., 2009). As shown in Tables 5.3 and 5.4, the Lewis-Acid (γ^+) components of the aggregate and asphalt binder specimens used in this study are in the range of 0.01 ergs/cm² to 0.90 ergs/cm².

CHAPTER VI

DISCUSSIONS

Testing protocols of direct contact angle measurements using the Sessile Drop (SD) device for aggregate and binder specimens were developed. The values of average contact angles of three different probe liquids on these specimens (Davis limestone, Snyder granite, Dolese Cooperton limestone, Hanson Davis rhyolite, Martin Marietta Mill Creek granite, Dolese Hartshorn limestone, Pryor limestone, and PG 64-22 asphalt binder) were measured following the testing protocols given in Chapter IV. The results of direct contact angle measurements with SD device were then used to calculate the surface free energy (SFE) components of aggregate and binder specimens. The results of the SFE calculations of aggregates and binders were given in Chapter V and compared to the results of similar materials in the literature in this chapter (Table 6.1 and Table 6.2).

Standard deviations of the contact angles as given in Table 5.1 for Davis limestone and Snyder granite are comparably higher than the standard deviations of the other samples (Dolese Cooperton limestone, Hanson Davis rhyolite, Martin Marietta Mill Creek granite, Dolese Hartshorn limestone, Pryor limestone). The standard deviations of the contact angles on Davis limestone and Snyder granite with water were 4.7° and 4.0° , respectively. Also, the standard deviations for Snyder granite specimen with ethylene glycol and diiodomethane were 3.9° and 3.8° , respectively. On the other hand, the contact angle tests on the other samples have revealed

standard deviations ranging from 0.6° to 2.6° as it can be seen in Table 5.1. The reason for these differences can be explained by the surface roughness levels of the aggregate specimens. As explained in Chapter IV, Snyder granite and Davis limestone specimens were polished with 1000 grade silicon carbide grits while the other aggregate samples were polished further using the 5 micron aluminum oxide powder in addition to the 1000 grade silicon carbide grit. The 5 micron aluminum oxide powder has smaller particle size than the 1000 grade silicon carbide grit. Since these samples were polished using a finer grade polishing material, they had smoother surfaces compared to Snyder granite and Davis limestone. In the SD method, the surface roughness of the material plays a vital role in contact angle measurements. Hence it can be stated that the higher levels of the surface roughness of Snyder granite and Davis limestone samples caused the higher standard deviations in contact angle measurements using the SD device as given in Table 5.1.

As shown in Table 5.3 in Chapter V, among all the aggregates tested in this study, the lowest and highest values of total SFE components are 34.66 ergs/cm² and 49.37 ergs/cm², respectively. These values are within the ranges of total surface energy components of typical geological materials in the literature such as clay and talc minerals as given in Table 6.1. On the other hand, the surface energy components of typical aggregates in the literature using the Universal Sorption Device (USD) testing method, also listed in Table 6.1, are significantly different, in some cases, than the same surface energy components of the aggregates tested using the SD device in this study, and the more energetic geological minerals (i.e., clay) tested using the SD, Column Wicking, Heat of Immersion methods in the literature. For instance, the base components from the USD measurements range from 259.0 to 782.7 ergs/cm². On the other hand, the ranges of base components for all the other materials (including the results from the SD) is from 0.2 to 39.5 ergs/cm².

Table 6-1 Surface free energy components of different geological materials in literature.

Material	γ^-	γ^+	γ^{AB}	γ^{LW}	γ^{Total}
	(ergs/cm ² or mJ/m ²)				
Davis Limestone ¹	10.12	0.05	1.35	36.26	37.61
Snyder Granite ¹	13.97	0.01	0.28	34.39	34.66
Montana talc ²	27.4	0.2	4.7	42.9	47.6
Vermont talc ²	28.4	0.1	3.4	44.6	48.0
Montmorillonite ³	33.4	2.3	17.3	42.4	59.8
Limestone ⁴	259.0	2.4	49.5	44.1	93.6
Limestone ⁵	540.7	13.0	168.0	51.9	219.9
Montana-ROM ⁶	14.5	0.2	3.3	53.4	56.7
Granite ⁷	782.7	43.6	368.9	56.3	425.2

¹Results from this study (Sessile Drop Method); ²Yildirim 2001 (Sessile Drop Method); ³Giese and van Oss 2002 (Column Wicking Method); ⁴Bhasin 2006 (Universal Sorption Device); ⁵Wasiuddin 2007 (Universal Sorption Device); ⁶Yildirim 2001 (Heat of Immersion); ⁷Lytton et al. 2005 (Universal Sorption Device).

There might be several possible causes for these major differences of the surface energy components of similar aggregates using the USD and SD testing approaches. One of the major differences between the USD and SD methods is the adopted equation for the calculation of the surface energy parameters. The USD method uses Equation 3.48 and the SD method employs Equation 3.23 (given in Chapter III). The major difference between these two equations is the equilibrium spreading pressure (π_e) term given in Equation 3.24. It is believed that the justification of using the π_e term should be investigated in detail.

Bhasin (2006) attempts to explain the reason for the use of the spreading pressure. The USD approach, employed by Bhasin (2006), Lytton et al. (2005), and others, assumes that aggregates,

such as limestone and granite, have high surface energies and thus the spreading pressure on the surfaces of these materials are greater than zero. This approach assumes that contact angles on high surface energy aggregates are zero. In other words, contact angles will not form on these materials, and the liquid drop will completely spread out over the surface of the aggregate.

On the other hand, literature review (i.e., Giese and van Oss, 2002; Yildirim, 2001) indicates that contact angle measurements on highly energetic minerals (i.e., clay) are non-zero. It should be realized that clay minerals are much more energetic materials than commonly used aggregates in pavement engineering. Therefore, Equation 3.23 (the Young-Dupre equation) should be used in its present form without any modifications. Van Oss (2002) clearly states that, *in all cases where finite contact angle occurs (where $\theta > 0^\circ$), there is no need to insert imaginary 'equilibrium spreading pressures' into Young-Dupre equation*. Wu (1982) claimed that if the contact angle is larger than 10° , the spreading pressure is negligible. As it can be seen very clearly from Table 5.1 that all of the contact angles measured in this study was finite and larger 10° .

Table 6-2 Surface energy components of PG 64-22 neat binder compared to results in the literature.

Asphalt Binder	γ^-	γ^+	γ^{AB}	γ^{LW}	γ^{Total}
	(ergs/cm ² or mJ/m ²)				
PG 64-22 ¹	2.82	0.12	1.15	35.38	36.53
PG 64-22 ²	1.02	0.01	0.05	29.95	30.07
AAF-1 ³	3.52	0.01	0.38	38.38	38.80

¹Results from this study (Sessile Drop Method); ² Lytton et al. 2005 (Wilhelmy Plate Method); ³ Bhasin 2006 (Wilhelmy Plate Method), AAF-1 is equivalent to PG 64-22.

The laboratory tests on PG 64-22 asphalt binder specimens indicate that the surface energy components obtained from the SD measurements are in close agreement with the results obtained

from the Wilhelmy Plate (WP) equipment (Table 6.2). Bhasin (2006) calculated the total surface energy of the PG 64-22 binder as 38.80 ergs/cm² while Lytton et al. (2005) came up with 30.07 ergs/cm² using the WP method, the test results from the SD method in this study on a similar material has revealed 36.53 ergs/cm² of total surface energy. The values of all other components of the surface energy calculated using the SD method were in agreement with the results obtained by Lytton et al. (2005) and Bhasin (2006). These similarities are resulted from the fact that, both SD and WP methods make use of the Young-Dupre equation without any modification and using the contact angle measurements. The only difference between the SD and the WP method is that in the WP method the contact angles are measured indirectly while the contact angles in the SD method are measured directly.

CHAPTER VII

CONCLUSIONS

A new sessile drop device was employed for direct measurements of contact angles on flat and smooth aggregate surfaces and asphalt binders. Large size bulk rock samples (from about 10cm to 30 cm in average diameter) of limestone, granite, and rhyolite from various rock quarries in Oklahoma and one binder type (PG 64-22) from Ergon, Muskogee, Oklahoma were obtained and subjected to newly developed sample preparation techniques for contact angle measurements. The sample preparation and testing protocols for contact angle measurements on the surfaces of aggregates, neat asphalt binder and asphalt binder mixed with Warm Mix Asphalt (WMA) additives were introduced. The sample preparation and testing processes are simple and require minimal training.

Using the Good-van Oss-Chaudhury (GVOC) approach, the surface energy components of aggregate and asphalt binder specimens were calculated by making use of the contact angles obtained from the Sessile Drop (SD) device. The contact angle results have shown small standard deviations (less than 2.6°) and the calculated surface energy components were in agreement with the results in the literature.

The aggregate specimens were subjected to various levels of polishing using different particle sizes of silicon and aluminum powder grits. Finer grade polishing materials resulted in smoother, lower roughness levels and thus smaller standard deviations of contact angle measurements.

The SFE components of the aggregate and asphalt binder samples in dry condition were calculated using the GVOC approach. As it was expected, the acidic components of all the materials were almost negligible (indicating a dry material) as opposed to the basic components. The surface energy components calculated using the contact angle measurements with the SD device in this study are comparable with the results from the studies conducted by Giese and van Oss (2002), Yildirim (2001) and Bargir et al. (2009). All these researchers used contact angles with GVOC approach without any modifications to the Young-Dupre equation. However, the comparison of the same results to the findings in Bhasin (2006), Wasiuddin (2007), and Lytton et al. (2005) shows that the surface energy components measured on aggregates with the USD and SD are significantly different from each other. In the USD method, the GVOC approach has been modified and the contact angle term was replaced by the spreading pressure term in spite of the fact that van Oss (2002), one of the pioneers of the GVOC approach, clearly stated that if finite contact angles occur, this approach should be used in its current form without any modifications. On the other hand, the results of this thesis study shows that all aggregates used in this study have yielded finite contact angles, in agreement with the results in the literature on some very surface energetic minerals like clays.

The comparison of the test results on asphalt binder specimens using the SD device and WP methods revealed a very close agreement. Furthermore, unlike the WP method, the contact angles from the SD device are obtained directly, and with much simpler sample preparation and testing processes.

This research study showed that the SD device is fully capable of performing direct contact angle measurements on flat surfaces such as aggregate and asphalt binders.

The SD device costs much less than the USD and the WP. The new equipment is accurate, reliable, practical, and economical, and it can easily be adopted in a materials laboratory for

contact angle measurements of aggregates and asphalt binders for determining the interfacial bonding strength using the surface energy approach. Testing protocols have been developed for aggregate and binder specimen preparations and contact angle measurements.

CHAPTER VIII

RECOMMENDATIONS

The differences in surface energy components calculated using the Sessile Drop (SD) device and Universal Sorption Device (USD) indicate that more research is needed for understanding the working principles between the two devices and the theoretical background leading to the calculations of surface energy components. These differences may be attributed to the spreading pressure term used in the universal sorption device testing approach and need to be investigated in detail.

The results of direct contact angle measurements using the SD showed that, surface roughness of the solid material plays a vital role in contact angle measurements. The results showed that, as the solid surface becomes smoother, more accurate and reliable contact angle measurements can be obtained. In other words, as the roughness level of the solid surface decreases, the standard deviation of contact angles becomes less. According to the sample preparation protocol given in this study, the polishing process leads to lower levels of roughness on aggregate surfaces. The finest grade polishing material used for Davis limestone and Snyder granite is 1000 grade silicon carbide grits. The more precise contact angles and less standard deviation were obtained on smoother surfaces which were obtained by using a finer grade polishing material such as 5 μ aluminum oxide powder. These results can be improved with finer grade polishing materials.

As a suggestion for future studies, the testing protocols for emulsions and powdered materials (i.e., clay minerals) for measuring direct contact angles using the SD device can be developed.

REFERENCES

Adamson, A.W., and Gast, A.P. (1997). "Physical Chemistry of Surfaces", 6th ed., John Wiley and Sons, New York.

American Road & Transportation Builders Association (2012). "Transportation and General Public F.A.Q.". Retrieved October 14, 2012, from <http://www.artba.org>.

Bangham, D.H. and R.I. Razouk (1937). "Adsorption and Wettability of Solid Surfaces." Transactions of the Faraday Society, Vol. 37, pp. 1459-1463.

Bargir, S., Dunn, S., Jefferson, B., Macadam, J., Parsons, S. (2009). "The Use of Contact Angle Measurements to Estimate the Adhesion Propensity of Calcium Carbonate to Solid Substrates in Water." Applied Surface Science, 255(9), 4873-4879.

Bhasin, A. and Little, D.N. (2007). "Characterization of Aggregate Surface Energy Using the Universal Sorption Device." *ASCE Journal of Materials in Civil Engineering*, 19(8), 634-641.

Bhasin, A. (2006). "Development of Methods to Quantify Bitumen-Aggregate Adhesion and Loss of Adhesion Due to Water." Ph.D. Dissertation, Texas A&M University, College Station, Texas.

Chaudhury, M.K., Short range and long range forces in colloid and macroscopic systems, Ph.D. Dissertation, SUNY, Buffalo, 1984.

Cheng, D. (2002). "Surface Free Energy of Asphalt-Aggregate Systems and Performance Analysis of Asphalt Concrete Base on Surface Free Energy," Ph.D. Dissertation, Texas A&M University, College Station, Texas.

Cheng, D., Little, D.N., Lytton, R.L. and Holste, J. (2002). "Use of Surface Free Energy Properties of the Asphalt- Aggregate System to Predict Moisture Damage Potential." *Journal of the Association of Asphalt Paving Technologists*, AAPT, Vol.71, 59-88.

Costanzo, P. M., Wu, W., Giese, R. F., & van Oss, C. J. (1995). "Comparison between Direct Contact Angle Measurements and Thin Layer Wicking on Synthetic Monosized Cuboid Hematite Particles." *Langmuir*, 11(5), 1827-1830.

Curtis, C.W. (1992). "Investigation of Asphalt-Aggregate Interactions in Asphalt Pavements." American Chemical Society, Fuel, 37, 1292-1297.

Curtis, C.W., Perry, L.M. and Brannan C.J. (1991). "Investigation of Asphalt-Aggregate Interactions and Their Sensitivity to Water." VTI Report 372A, Part 4. Swedish National Road and Transport Research Institute.

Elphingstone, G.M., Jr., (1997). "Adhesion and Cohesion in Asphalt-Aggregate Systems". Ph.D. Dissertation, Texas A&M University.

Eustathopoulos, N.; Nicholas, M.G. and Drevet B. (1999). "Wettability at high temperatures." Oxford, UK: Pergamon. ISBN 0-08-042146-6

Extrand, C. W. (2003). "Contact Angles and Hysteresis on Surfaces with Chemically Heterogeneous Islands". *Langmuir*, Vol.19(9), 3793-3796

Fowkes, F.M. (1963). "Additivity of intermolecular forces at interfaces. I. Determination of the contribution to surface and interfacial tensions of dispersion forces in various liquids." *Journal of Physical Chemistry*, Vol. 67, 2538-2541.

Fowkes, F.M. (1964). "Attractive Forces at Interfaces." *Industrial and Engineering Chemistry*, Vol. 56(12), pp. 40-52.

Fowkes, F.M. (1987). "Role of Acid-Base Interfacial Bonding in Adhesion." *Journal of Adhesion Science and Technology*, Vol. 1(1), pp. 7-27.

Giese, J., R. F., et al. (1996). "Surface and Electrokinetic Properties of Clays and Other Mineral Particles, Untreated and Treated with Organic or Inorganic Cations." *Journal of Dispersion Science and Technology*, Vol. 17(5), pp. 527-547.

Giese, R.F. and van Oss, C.J. (2002). "Colloid and Surface Properties of Clays and Related Materials." Marcel Dekker, Inc., New York.

Girifalco, L.A. and R.J. Good. (1957). "A Theory for Estimation of Surface and Interfacial Energies. I. Derivation and Application to Interfacial Tension." *Journal of Physical Chemistry*, Vol. 61, pp. 904-909.

Good, R.J. (1966). "Physical Significance of Parameters γ_c , γ_s , and Φ that Govern Spreading on Adsorbed Films". S. C. I. Monograph 25(25), pp. 328-350.

Good, R.J. (1992). "Contact Angle, Wetting and Adhesion: A Critical Review". *Journal of Adhesion Science and Technology*, Vol 6(12), pp. 1269-1302.

Groszek, A. (1962). "Preferential Adsorption of Normal Hydrocarbons on Cast Iron." *Nature*, 196 (4854), 531-&.

Gugliotti, M. (2004). "Tears of Wine." *Journal of Chemical Education*, 81.1, 67-68.

Hall, C., Hoff, W.D. (2002). "Water Transport in Brick, Stone, and Concrete." Spon Press, London.

Hefer, A.W., Bhasin, A., and Little, D.N. (2006). "Bitumen Surface Energy Characterization Using Contact Angle Approach." *ASCE Journal of Materials in Civil Engineering*, 18(6), 759-767.

Holmberg, K. (2002). "Handbook of Applied Surface and Colloid Chemistry." Wiley and Sons, New York.

Howson, J., Masad, E.A, Bhasin, A., Branco, V.C., Arambula, E., Lytton, R., and Little, D. (2007). "System for the evaluation of moisture damage using fundamental material properties." TxDOT Report Number 0-4524-2. FHWA, Texas Transportation Institute, Texas A&M University, College Station, Texas.

Kanitpong, K. and Bahia, H.U. (2005). "Relating Adhesion and Cohesion of Asphalts to the Effects of Moisture on Laboratory Performance of Asphalt Mixtures." *Transportation Research Record No. 1901*, Transportation Research Board, Washington, D.C., 33-43.

Kringos, N. and Scarpas, A. (2008). "Physical and Mechanical Moisture Susceptibility of Asphalt Mixtures." *International Journal of Solids and Structures*, Vol. 45, 2671-2685.

Lam, C.N.C., et al. (2002). "Measuring Contact Angle, in Handbook of Applied Surface and Colloid Chemistry." John Wiley & Sons, New York.

Lobato, E.M.C."Determination of Surface Free Energies and Aspect Ratio of Talc." Ms. Thesis, Virginia Polytechnic Institute and State University, Blacksburg, Virginia, 2004.

Lu, Q. and Harvey, J.T. (2008). "Investigation of Conditions for Moisture Damage in Asphalt Concrete and Appropriate Laboratory Test Methods." Research Report No.: UCPRC-RR-2005-15, California Department of Transportation.

Lytton, R.L., Masad, E., Zollinger, C., Bulut, R., and Little, D.N. (2005). "Measurement of Surface Energy and Its Relationship to Moisture Damage," TxDOT Report Number 0-4524-2. FHWA, Texas Transportation Institute, Texas A&M University, College Station, Texas.

Masad, E., Zollinger, C., Bulut, R., Little, D.N., and Lytton, R.L. (2006). "Characterization of Moisture Damage Using Surface Energy and Fracture Material Properties." *Journal of the Association of Asphalt Paving Technologists*, AAPT, Vol. 75, 713-732.

Petrucchi, R.H., Harwood, W.S., Herring, G.E., and Madura, J. (2007). “General Chemistry: Principles & Modern Applications.” Prentice Hall, Upper Saddle River, New Jersey.

Pinto, I., Kim, Y.K., and Ban, H. (2009). “Moisture Sensitivity of Hot-Mix Asphalt (HMA) Mixtures in Nebraska – Phase II.” NDOR Research Project Number: MPM-04, Nebraska Department of Roads.

Puckette, J. (2011). “Personal Communication.” Department of Geology, Oklahoma State University, Stillwater, Oklahoma.

Rulison, C. (1996). "So you Want to Measure Surface Energy?" KRÜSS technical note TN306e

Shang, J., Flury, M., Harsh, J.B., Zollars, R.L. (2008). “Comparison of Different Methods to Measure Contact Angles of Soil Colloids.” *Journal of Colloid and Interface Science*, Vol. 328, Issue 2, 299-307.

Sharfrin, E., Zisman, William A. (1960). "Constitutive relations in the wetting of low energy surfaces and the theory of the retraction method of preparing monolayers". *The Journal of Physical Chemistry*, 64 (5): 519–524.

U.S. Department of Transportation, Federal Highway Administration, *Highway Statistics*, Washington, D.C. http://www.bts.gov/publications/national_transportation_statistics. Accessed October 14, 2012.

van Oss, C.J., et al. (1988). “Interfacial Lifshitz-van der Waals and Polar Interactions in Macroscopic Systems.” *Chemical Reviews*, Vol. 88, pp. 927-941.

van Oss, C.J. (1994). "Interfacial Forces in Aqueous Media." Marcel Dekker, Inc., New York.

van Oss, C.J. (2002). "Use of the Combined Lifshitz-van der Waals and Lewis Acid-base Approaches in Determining the Apolar Contributions to Surface and Interfacial Tensions and Free Energies." *Journal of Adhesion Science and Technology*, Vol. 16, 669-677.

van Oss, C.J., Chaudhury, M.K., and Good, R.J. (1987). "Monopolar surfaces." *Journal of Protein Chemistry*, Vol. 5, 385-405.

Wasiuddin, N. M. (2007). "Effect of Additives on Surface Free Energy Characteristics of Aggregates and Binders in Hot Mix Asphalt." Ph.D. Dissertation, University of Oklahoma, Norman, Oklahoma.

Wasiuddin, N.M., Zaman, M., and O'Rear, E.A. (2008). "Effect of Sasobit and Aspha-Min on Wettability and Adhesion Between Asphalt Binders and Aggregates." Transportation Research Record No. 2051, Transportation Research Board, Washington, D.C., 80-89.

Wilber, G.G. (2011). "Personal Communication." School of Civil and Environmental Engineering, Oklahoma State University, Stillwater, Oklahoma.

Wu, S., (1982). "Interfacial Thermodynamics in Polymer Interface and Adhesion." Marcel Dekker, New York.

Yancey, T.E. (2006). "Personal Communication." Department of Geology and Geophysics, Texas A&M University, College Station, Texas.

Yildirim, I. (2001). "Surface Free Energy Characterization of Powders." Ph.D. Dissertation,
Virginia Polytechnic Institute and State University, Blacksburg, Virginia.

APPENDICES

APPENDIX A: CALIBRATION OF THE SESSILE DROP DEVICE

The FTA 1000B goiometer was employed to measure contact angles on both aggregates and asphalt binder. The device includes a high resolution camera which takes pictures of the samples with the sessile drop dispensed from a needle and sends the pictures to the software for processing. The magnification has to be adjusted to obtain better snapshots of liquid-solid interface. The quality of these pictures directly affect the presicion of the contact angles calculated by the FTA software. Focus, image clarity, and isolation from mechanical vibration can cause inaccurate contact angle results. To achieve more precise results, the device was calibrated on a frequent base by the procedure given below.

In this process, distilled water was used as the probe liquid. About 12 μL of distilled water was dispensed as pendant drop. The snapshots of the drop were taken and sent to the software. Certain physical parameters of the drop such as volume, diameter, radius of curvature, and interfacial tension were measured by the software. The actual value of interfacial tension (IFT) of the water is 72.00 mN/m at the room temperature (Table 3.1). However as it can be seen in Figure A.1, the device measured 70.89 mN/m before the calibration.

The calibration can be conducted in three different ways (see Figure A.2). In this study, the calibration of the device was performed by matching the actual and measured IFT values. Once these values are entered, the calibration is completed by clicking the apply button. The difference in the results is shown in Figure A.3. The physical parameters of the pendant drop are now closer

to the theoretical values. To illustrate it quantitatively, the pendant volume has increased from 12.41 μL to 12.70 μL after the magnification of the FTA device was calibrated.

These differences in the readings of physical parameters of the pendant drop has a direct impact on contact angle values.

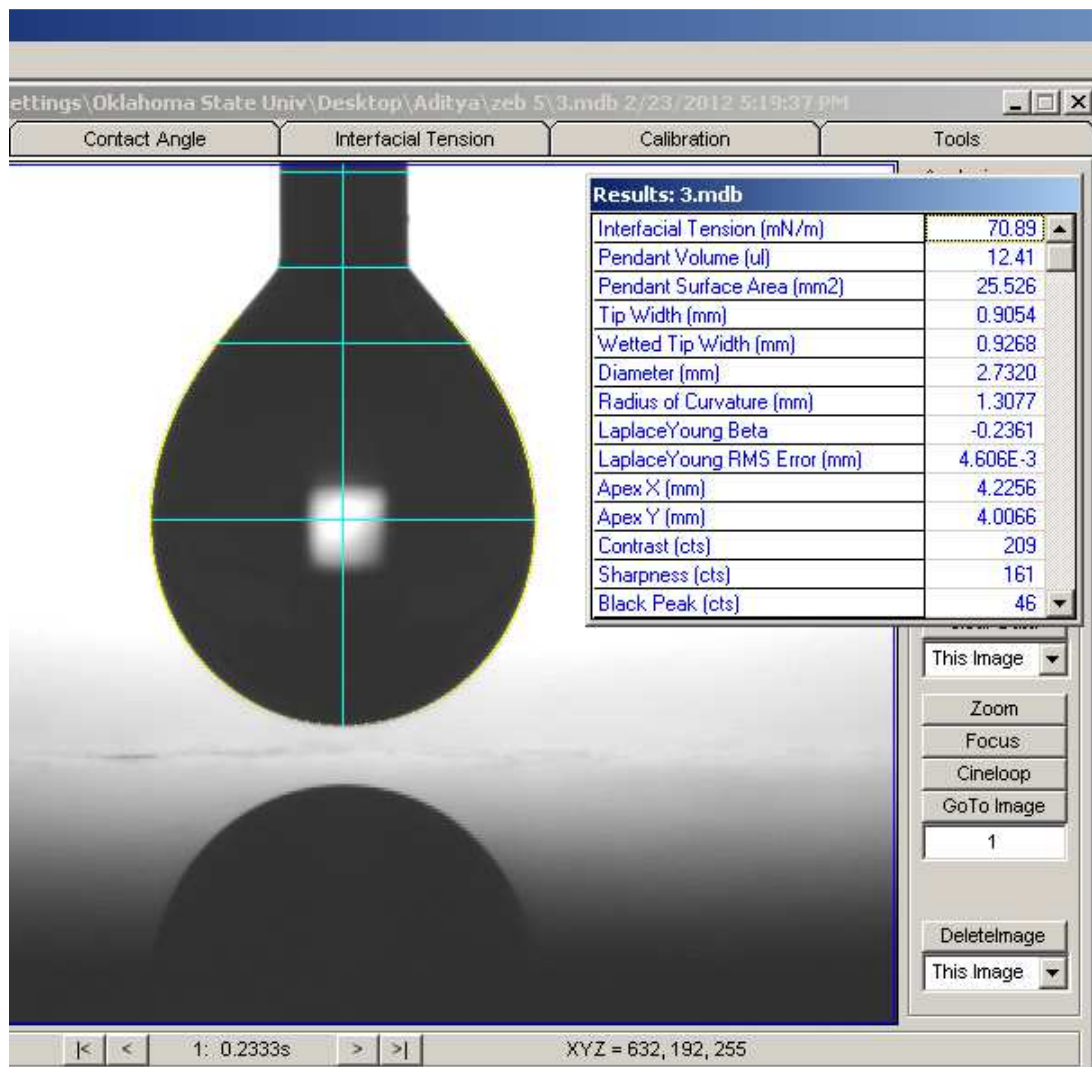


Figure A-4 IFT results before the calibration

Add Row

Magnification Calibration

Calibration by Known Linear Distance

Actual Distance (mm):	0.9140	Apply
Measured Distance (mm):	0.9180	

Calibration by Known IFT

Actual IFT (mN/m):	72.00	Apply
Measured IFT (mN/m):	70.89	

Calibration by Directly Setting nm/pixel

Magnification (nm/pixel):	12797.7	Apply

Set magnification

Figure A-5 The calibration window

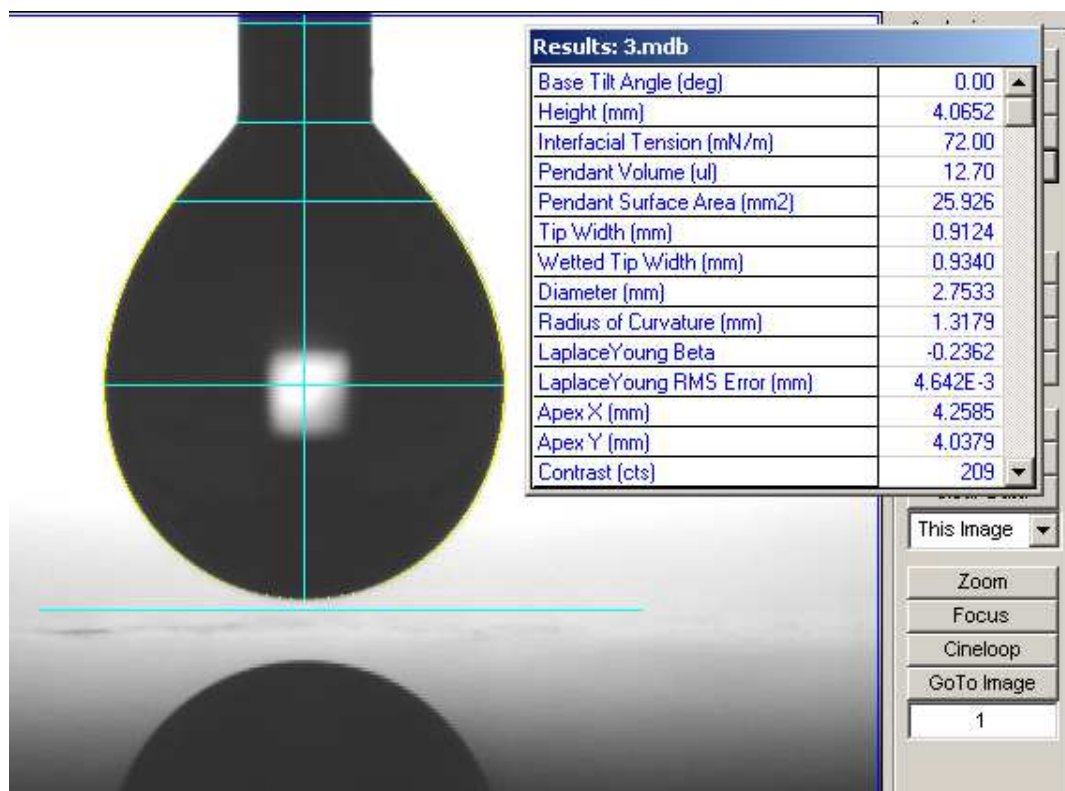


Figure A-6 IFT results after the calibration

APPENDIX B: CONTACT ANGLE TEST RESULTS USING THE TESTING PROTOCOL
DEVELOPED IN THIS STUDY

Tables in this appendix include the contact angle measurement test results using the testing protocol developed in this research study. Results of surface energy calculations using the measured contact angles are also given. The samples used in this study are namely:

Davis Limestone

Snyder Granite

Dolese Copperton Limestone

Hanson Davis Rhyolite

Martin Marietta Mill Creek Granite

Dolese Hartshorn Limestone

Pryor Stone (Pryor Limestone)

PG 64-22 neat binder from Ergon, Muskogee, Oklahoma
PG 64-22 neat binder from Ergon,
Muskogee, Oklahoma

All contact angle results presented in this study are in the units of degrees ($^{\circ}$) and surface energy components are in the units of ergs/cm^2 (mJ/m^2).

Table B.1 Final contact angle results with PG 64-22 neat binder.

Trial Number	Ethylene Glycol	DIM	Water
1	68.5	48.0	93.0
2	70.5	47.5	92.0
3	69.0	46.0	94.0
4	73.5	49.0	94.5
5	73.5	50.0	91.5
6	68.0	47.5	93.0
Std. Dev.	2.5	1.4	1.1
Average	70.5	48.0	93.0

Table B.2 Final contact angle results on aggregate samples with Distilled Water.

Sample	1 st Set	2 nd Set	3 rd Set	Average
Dolese Copperton I	57.0	54.9	52.8	54.9
Dolese Copperton II	51.1	52.0	52.9	52.0
Dolese Copperton III	67.1	63.5	66.4	65.7
Hanson Davis I	51.7	53.5	54.5	53.2
Hanson Davis II	61.7	61.5	59.5	60.9
Martin Marietta Mill Creek I	48.0	46.2	42.0	45.4
Martin Marietta Mill Creek II	55.6	59.2	58.1	57.6
Martin Marietta Mill Creek III	45.3	45.0	44.5	44.9
Dolese Hartshorn	62.0	65.1	65.6	64.2
Pryor Stone Pryor I	58.2	55.3	58.3	57.2
Pryor Stone Pryor II	61.3	60.0	60.6	60.6
Davis Limestone	79.6	78.1	80.4	79.4
Snyder Granite	74.5	73.5	75.8	74.6

Table B.3 Final contact angle results on aggregate samples with Diiodomethane.

Sample	1 st Set	2 nd Set	3 rd Set	Average
Dolese Copperton I	29.2	29.7	30.3	29.8
Dolese Copperton II	43.5	44.0	44.3	43.9
Dolese Copperton III	40.8	41.7	42.7	41.7
Hanson Davis I	38.9	37.4	39.5	39.4
Hanson Davis II	45.9	44.4	44.6	45.0
Martin Marietta Mill Creek I	45.7	47.4	48.4	47.2
Martin Marietta Mill Creek II	48.1	49.7	49.7	49.2
Martin Marietta Mill Creek III	42.0	42.6	40.8	41.8
Dolese Hartshorn	40.2	43.9	44.4	42.8
Pryor Stone Pryor I	43.2	43.6	45.6	44.1
Pryor Stone Pryor II	31.9	35.3	37.0	34.7
Davis Limestone	47.1	47.7	44.5	46.4
Snyder Granite	50.4	49.5	49.5	49.8

Table B.4 Final contact angle results on aggregate samples with Ethylene Glycol.

Sample	1 st Set	2 nd Set	3 rd Set	Average
Dolese Copperton I	28.4	28.2	26.7	27.7
Dolese Copperton II	34.9	37.9	37.2	36.7
Dolese Copperton III	41.3	46.4	43.8	43.8
Hanson Davis I	30.4	30.5	27.9	29.4
Hanson Davis II	32.3	34.3	33.1	33.2
Martin Marietta Mill Creek I	30.3	28.3	26.5	28.4
Martin Marietta Mill Creek II	39.2	40.6	38.5	39.4
Martin Marietta Mill Creek III	32.3	34.3	33.1	33.2
Dolese Hartshorn	35.3	29.3	29.2	31.3
Pryor Stone Pryor I	28.9	27.8	27.3	28.0
Pryor Stone Pryor II	18.2	17.6	20.4	18.7
Davis Limestone	60.5	63.4	61.3	61.7
Snyder Granite	56.8	59.6	59.5	58.6

Table B.5 The Surface Free Energy components of all samples.

Sample	γ^-	γ^+	γ^{AB}	γ^{LW}	γ^{Total}
	(ergs/cm ² or mJ/m ²)				
Dolese Copperton I	22.97	0.16	3.86	44.30	48.17
Dolese Copperton II	31.51	0.13	4.03	37.58	41.61
Dolese Copperton III	16.95	0.09	2.52	38.73	41.24
Hanson Davis I	26.26	0.31	5.66	39.91	45.57
Hanson Davis II	18.53	0.61	6.71	37.03	43.74
Martin Marietta Mill Creek I	36.98	0.42	7.89	35.84	43.73
Martin Marietta Mill Creek II	25.62	0.31	5.60	34.74	40.33
Martin Marietta Mill Creek III	39.42	0.07	3.44	38.69	42.13
Dolese Hartshorn	14.02	0.78	6.62	38.16	44.78
Pryor Stone Pryor I	21.05	0.73	7.85	37.48	45.33
Pryor Stone Pryor II	14.34	0.90	7.20	42.16	49.36
Davis Limestone	10.12	0.05	1.35	36.26	37.61
Snyder Granite	13.97	0.00	0.28	34.39	34.66
PG 64-22 Neat Binder	2.82	0.12	1.15	35.38	36.53

Table B.6 Contact angle results on PG 64-22 neat binder with Distilled Water.

Trial Number	Set I	Set II	Set III
1	93.0	94.5	95.0
2	88.0	92.0	94.5
3	92.0	95.0	93.0
4	91.5	93.0	94.0
5	89.5	91.5	91.5
6	92.5	93.0	93.5
7	88.0	92.5	90.0
8	85.0	89.0	89.5
9	87.5	92.5	90.5
10	81.0	94.0	91.0
11	86.5	95.5	91.5
12	82.0	94.0	88.0
13	87.5	92.5	92.5
14	90.0	93.0	93.0
Std. Dev.	3.7	1.6	2.0
Average	88.1	93.0	92.0

Table B.7 Contact angle results on PG 64-22 neat binder with Diiodomethane.

Trial Number	Set I	Set II	Set III
1	46.0	48.0	47.0
2	46.0	47.5	49.5
3	44.5	46.0	50.0
4	47.0	49.0	51.0
5	48.0	50.0	47.5
6	45.0	47.5	45.5
7	47.0	48.0	48.0
8	44.0	47.0	50.5
9	43.5	47.5	51.0
10	43.0	46.5	51.0
11	46.0	47.0	49.0
12	44.0	49.5	48.5
13	42.0	50.5	50.0
14	41.0	51.0	52.0
Std. Dev.	2.0	1.5	1.8
Average	44.8	48.2	49.3

Table B.8 Contact angle results on PG 64-22 neat binder with Ethylene Glycol.

Trial Number	Set I	Set II	Set III
1	78.5	68.5	76.5
2	83.5	70.5	76.5
3	79.5	69.0	74.0
4	85.0	73.5	72.5
5	84.0	73.5	75.5
6	80.0	68.0	77.0
7	75.5	70.0	78.0
8	75.0	72.5	79.5
9	76.0	70.5	76.0
10	74.5	73.0	75.0
11	75.5	71.0	73.5
12	73.5	68.0	72.0
13	71.0	68.5	71.0
14	66.0	70.0	69.0
Std. Dev.	5.2	2.0	2.9
Average	77.0	70.5	74.7

VITA

Murat Koc

Candidate for the Degree of

Master of Science

Thesis: DEVELOPMENT OF TESTING PROTOCOLS FOR DIRECT
MEASUREMENTS OF CONTACT ANGLES ON AGGREGATE AND
ASPHALT BINDER SURFACES USING A SESSILE DROP DEVICE

Major Field: Civil & Environmental Engineering

Biographical:

Education:

Completed the requirements for the Master of Science in Civil & Environmental
Engineering at Oklahoma State University, Stillwater, Oklahoma in May, 2013.

Completed the requirements for the Bachelor of Science in Civil Engineering at
Bogazici University, Istanbul, Turkey in 2010.